UCRL 2339

UNCLASSIFIED

UNIVERSITY OF CALIFORNIA

Radiation Laboratory

TWO-WEEK LOAN COPY

This is a Library Circulating Copy which may be borrowed for two weeks. For a personal retention copy, call Tech. Info. Division, Ext. 5545

BERKELEY, CALIFORNIA

DISCLAIMER

This document was prepared as an account of work sponsored by the United States Government. While this document is believed to contain correct information, neither the United States Government nor any agency thereof, nor the Regents of the University of California, nor any of their employees, makes any warranty, express or implied, or assumes any legal responsibility for the accuracy, completeness, or usefulness of any information, apparatus, product, or process disclosed, or represents that its use would not infringe privately owned rights. Reference herein to any specific commercial product, process, or service by its trade name, trademark, manufacturer, or otherwise, does not necessarily constitute or imply its endorsement, recommendation, or favoring by the United States Government or any agency thereof, or the Regents of the University of California. The views and opinions of authors expressed herein do not necessarily state or reflect those of the United States Government or any agency thereof or the Regents of the University of California.

UCRL-2339
Unclassified--Chemistry Distribution

UNCLASSIFIED

UNIVERSITY OF CALIFORNIA

Radiation Laboratory

Contract No. 7405-eng-48

THERMAL CONDUCTIVITY OF GASES AT HIGH TEMPERATURES

Albert Joel Rothman

(Thesis)

January, 1954

Berkeley, California

TABLE OF CONTENTS

	Page
Abstract	8
I. Introduction and Theory	9
A. Previous Investigations	10
1. Hot Wire	10
2. Parallel Plates	11
3. Spheres	11
4. Concentric Cylinders	11
B. Selection of Conductivity Cell	13
C. Theory	15
D. Theory of Measurement and Calculation	18
1. Cell Constant	18
2. Effect of Pressure	19
3. Radiation and Support Conduction	20
E. Gas Mixtures	21
II. Experimental	22
A. Equipment	22
1. Silver Cell	22
2. Furnace	24
3. Temperature Controls	30
4. Loading and Evacuation System	35
5. Cell Heating Circuits	37
6. Temperature Measurement	37
B. Procedure	40
1. Gas Measurements	40
2. Gas Mixtures	41
3. High Vacuum Runs	42
4. Pressure Runs	42

TABLE OF CONTENTS

(Page 2)

	Page
III. Results	43
IV. Discussion	65
A. Corrections	65
1. Vacuum Correction	65
2. Pressure Effects	67
(a) Convection	67
(b) Accommodation - Temperature Jump Effect	69
3. Effect of Temperature Gradient (Δt)	70
B. Conductivities of Gases	73
1. Air	73
2. Nitrogen	73
3. Carbon Dioxide	77
4. Argon	78
5. Helium	79
6. Nitrogen-Carbon Dioxide Mixtures	80
C. Evaluation and Conclusion	82
1. Random Errors	82
(a) Cell Constant	82
(b) Temperature	82
(c) Thermocouple Calibrations	82
(d) Heat Input	83
(e) Vacuum Corrections	83
(f) Pressure Correction	83
2. Reliability of Cell and Data	83
3. Suggested Conductivity Values for Nitrogen and Carbon Dioxide	85

TABLE OF CONTENTS

(Page 3)

4. Suggestions for Improvement 87

(a) Corrosion 87

(b) Thermocouples 88

(c) Convection 89

(d) De-Gassed Silver 89

(e) Flange Design 89

(f) Suspension of Emitter 90

V. Nomenclature 91

VI. References 93

VIII. Appendix 96

A. Gases Used 96

B. Measurement of Cell Dimensions 96

C. Calculation of Cell Constant 99

D. Sample Run and Calculations 101

E. Calibration of Thermocouples 101

F. Derivation of Accommodation-Temperature Jump Equation 101

1. Derivation Using Gregory's Equation 101

2. Derivation from the Temperature Jump Equation 105

G. Calculation of Conduction Across Supports 106

Acknowledgment 115

LIST OF FIGURES

Figure Number	Description	Page
1	Thermal Conductivity Cell Assembly	23
2	Constant Temperature Furnace	25
3a, b	Photographs of Equipment	26, 27
4	Electric Furnace Wiring Circuits	29
5	Temperature Controller, Power Supply	31
6	Temperature Controller, Pre-amplifier	32
7	Temperature Controller, Amplifier	33
8	Platinum Resistance Thermometer	34
9	Flow System Schematic	36
10	Electric Heating and Measuring Circuit	38
11	Thermal Conductivity of Air, Various Investigators	55
12	Thermal Conductivity vs. Temperature, Nitrogen	56
13	Thermal Conductivity vs. Temperature, Nitrogen, Various Investigators	57
14	Thermal Conductivity vs. Temperature, Carbon Dioxide	58
15	Thermal Conductivity vs. Temperature, Carbon Dioxide, Various Investigators	59
16	Thermal Conductivity vs. Temperature, Argon	60
17	Vacuum Runs $q/\Delta t$ vs. T^3	61
18	Pressure Effect $\Delta t/q$ vs. $1/P$	62
19	Thermal Conductivities of Nitrogen-Carbon Dioxide Mixtures	63
20	Thermal Conductivities of Nitrogen-Carbon Dioxide Mixtures (Keyes)	64
21	Cell Dimensions	109
22	E.M.F. vs. Temperature, Chromel-Alumel Standard Thermocouple	110
23	dE/dt vs. Temperature, Chromel-Alumel Standard Thermocouple	111

LIST OF FIGURES

(Page 2)

Figure Number	Description	Page
24	E vs. Temperature, Platinum-Platinum Rhodium Standard Thermocouple	112
25	dE/dt vs. Temperature, Platinum-Platinum Rhodium Standard Thermocouple	113
26	Conduction Across Support	114

LIST OF TABLES

Table	Title	Page
I	Experimental Data	45
II	Thermal Conductivity of Air at 0°C	52
III	Thermal Conductivity of Argon	53
IV	Accommodation Coefficients	54
V	Suggested Conductivities - Nitrogen and Carbon Dioxide	86
VI	Cell Dimensions	98
VII	Cell Constants	100
VIII	Sample Experimental Run	102
IX	Sample Calculation	104

THERMAL CONDUCTIVITY OF GASES AT HIGH TEMPERATURES

Albert J. Rothman

Radiation Laboratory and Department of Chemistry and Chemical Engineering
University of California
Berkeley, California

ABSTRACT

Apparatus suitable for measuring thermal conductivities of gases from 30°C to 800°C has been designed and operated successfully. The apparatus consists primarily of a conductivity cell formed of a pair of concentric silver cylinders, a constant-temperature furnace, and suitable control and measuring equipment. Conductivity values were obtained for nitrogen, carbon dioxide, and mixtures of the two at five or six temperatures from 50°C to 775°C. In addition, conductivities of argon were measured from 50°C to 680°C, and those of air and helium at 40°C and 680°C respectively. The results lie in the range of most investigators' values at all temperatures. Experimental uncertainty is about one percent, except for data at the two highest temperatures, 680°C and 775°C, which are estimated to be 2.5% and 3% high respectively. These errors were caused by the formation of gas bubbles on the silver surfaces above 600°C which reduced the annular spacing between the cylinders. The largest radiation correction required was 8%. Approximate accommodation coefficients were obtained for air, nitrogen, carbon dioxide, argon, and helium on silver.

I. INTRODUCTION AND THEORY

Thermal conductivity values for gases are essential in making calculations for conductive and convective heat transfer. Even at higher temperatures, where radiation becomes more effective, convected heat flow still represents a significant mechanism in the transmission of heat. To calculate convective effects, thermal conductivities must be known to a reasonable degree of accuracy. At present there exist few data at 400°C and almost none above that temperature. Reliable prediction of conductivities at high temperatures has not been possible using kinetic theory or modifications thereof. A few recent investigators[4,5,9,13,22] have attempted with some success to adapt the theory of non-uniform gases to predict the variation of conductivity with temperature. However, extensive conductivity measurements at widely varying temperatures are needed to test their theories.

In addition to their practical value, high temperature conductivity measurements may ultimately prove to be of value in clarifying the mechanism of energy transfer in gaseous molecular collisions.

The primary object of the present research was to design and develop a cell and auxiliary equipment suitable for measuring conductivities of gases up to moderately high temperatures (800°C). In order to check the operation of the equipment, data were to be obtained both for pure gases and for a mixture of two gases.

A. Previous Investigations.

Among the various devices which have been used are the hot wire cell, parallel plates, concentric spheres, and concentric cylinders.

1. Hot Wire.

The hot wire type of apparatus consists of a central heated wire which gives up its heat radially to a surrounding layer of gas contained in a cylindrical container. Pioneer measurements in a simple cell like this were carried out in 1840 by Andrews.[1] Schleiermacher[50] considerably improved the cell by using a pair of potential leads across the center portion of the hot wire, thus somewhat reducing the error caused by axial conduction of heat. Another scheme for reducing end effects was to use a pair of cells identical except in length, and by subtracting the two results the end effects were presumably eliminated.[7,17,43] The idea was further developed by Gregory and Archer[16] who used two such apparatus pairs with different cylinder diameters and corrected for convection by extrapolating to small diameters. Another innovation developed by Gregory was to make conductivity measurements at various pressures below atmospheric and to extrapolatethe results to infinite pressure in order to eliminate the effects of temperature jump and convection.[14]

Taylor and Johnston[56] used a carefully designed potential lead type of cell suitable for precise low temperature measurements.

Stops[52,54] also used a simple potential lead type of hot wire cell and made measurements up to 1000°C. However, his corrections for end effect and radiation were quite high (up to 20%).

The usual hot wire cells have utilized a long thin wire to approximate a mathematically infinite cylinder. Kannuluik and Martin,[28] on the other hand, used a relatively thick wire and analytically solved the heat conduction equation for such a case

to calculate the gas conductivity.

2. Parallel Plates.

Conceptually the simplest method consists in heating a flat plate and measuring the temperature difference between it and a plate parallel to it. Parallel plates were first used by Christiansen.[10] A number of investigators improved the apparatus somewhat, but Hercus and Laby[20] enhanced the apparatus considerably by using "guard rings" to minimize heat flow from the edges of the plates. Hercus and Sutherland[21] and more recently Ubbink and de Haas[57] utilized this type of cell and obtained good data.

3. Spheres.

Spheres were used by Kundt and Warburg[35] and by a number of other investigators up to about 1909, but were abandoned because of difficulties in obtaining good boundary conditions of spherical symmetry.

4. Concentric Cylinders.

The hot wire method may be said to utilize concentric cylinders, but the term is used here to refer more specifically to cylinders of approximately the same diameter with a relatively small annular space between them. Many early investigators used this type of apparatus, among whom Stefan[51] is the most noteworthy. He maintained a thin layer of gas between cylinders (as is done in the present investigation) to increase the gaseous conduction relative to the radiation and so reduce the percentage radiation correction.

Cylinders had not been used extensively for a period of about 30 years when, in 1950, Keyes and Sandell[32] used one well-designed to essentially eliminate convection and reduce radiation. Consequently, their design would have been suitable for measuring con-

ductivity at high temperatures, although they designed and operated their equipment up to only 400°C. They, too, used a thin annulus (0.025") between two large cylinders to reduce convection, particularly at the high pressures at which they made measurements on steam. They blocked the heat flow from the upper end of their cylinders by interposing a heated guard block. At the lower end they were able to calculate the heat flow as for a pair of parallel plates.

Glassman and Bonilla[65] constructed a concentric cylinder type of apparatus, in which the outer cylinder was electrically heated and the inner one (fused quartz) was cooled by means of a high velocity air stream. By using a transparent tube in this manner, they stabilized their radiation correction.

B. Selection of Conductivity Cell.

In order to choose a suitable device for measuring conductivity at high temperatures, considerations were made as follows:

1. Although simple in principle, it is difficult to provide adequate heat guards for the parallel plate type of cell since the complete periphery must be guarded. In addition, it is possible but awkward to enclose the plates so that measurements may be made at high vacua, which measurements are necessary to correct for radiation.*

2. Concentric spheres would be geometrically simple forms to use, but difficulties appear in accurately spacing them and bringing out the heater leads without disturbing the symmetry.

3. The hot-wire type of cell has been extensively used, and with undoubted success. However, the hot wire must be used as its own resistance thermometer, and therefore must be carefully placed to minimize strains due to thermal expansion. It is well known that the resistance changes markedly when the wire is strained. Also, endwise conduction and lack of temperature uniformity along the wire length offer a problem. Furthermore, it is difficult to maintain a desirably small annular space between inner and outer cylinders when a fine wire is used, and still to keep the wire free from strain.

---

* However, recently Michels and Botzen[41] described a cell of this type for high pressure, low temperature use. No data have yet been reported, but with a number of modifications the cell might be useful for high temperature work.

4. It appears that the heavier concentric cylinder type of apparatus, similar to that used by Keyes and Sandell[32] offers the advantage of independent temperature measuring devices, the possibility of accurate centering using a narrow annulus, and elimination of the need for accurate calibration and recalibration of a central heater wire.

C. Theory.

Maxwell[40] and Boltzmann[2] established the fundamental equations of kinetic theory relating thermal conductivity, viscosity, and diffusion coefficient. General solution of the equations were first carried out independently by Chapman[8] and Enskog.[11]

Simplified application of kinetic theory to rigid, elastic spherical molecules yields the relationship[9]

$$k = \underline{f}\ \eta\ c_v, \quad \text{where} \quad \underline{f} = 1.0. \qquad (1)$$

However, experimentally one finds that the constant of proportionality, $\underline{f}$, is closer to 2.5 than to 1.0. By taking into account the persistence of molecular velocity after impact, the fact that the most rapid molecules also have the greatest energy, and that molecules differing in speed also have different free path lengths, it has been shown[9] that $\underline{f} = 2.5$. The theory has been developed on the basis of a gas in equilibrium, while in fact, the occurrence of transport phenomena implies a non-equilibrium condition. Consequently, the theory can give only an approximation to the facts. Other proportionality constants have been derived for other molecular models, such as rough spheres of constant radius, wherein $\underline{f}$ = 1.71 to 1.87, the exact value depending upon the distribution of mass in the molecule.[9]

Eucken[12] rendered the theory more practicable by splitting the conductivity into translational and internal energy terms. He thereby obtained:

$$k = (1/4)(9\gamma - 5)\eta\ c_v \qquad (2)$$

Chapman and Cowling (loc. cit.) criticized his assumption that translational energy exchange takes place independently of the internal energies. In addition they pointed out that even if this assumption were correct, he should have used the mean free path as related to self-diffusion, rather than that related to viscosity, since internal

energy would then be transferred by diffusion of molecules from one place to another. With these considerations in mind, Chapman and Cowling wrote

$$k = \left\{(15/4)(\gamma - 1) + (1/2)u_{11} \quad (5 - 3\gamma)\right\} \eta c_v \qquad (3)$$

where $u_{11} = \frac{D_{11}\rho}{\eta} > 1$ and depends upon the type of molecules (whether smooth rigid spheres, or force-centers, etc.)

By assuming that vibrational energy and in most cases the rotational energy (where the rotational quanta are large) are transferred only rarely by collision, and therefore chiefly by diffusion, Schaefer[47] improved Eucken's relation. Schaefer also employed a parameter involving the dipole moment and was able to correlate $k/\eta c_v$ for polar substances fairly well, in contrast to Eucken's method.

Hirschfelder and coworkers,[22-24] assuming inverse sixth-power attraction and twelfth-power repulsion force laws between molecules, evaluated the collision integrals set up by Chapman and Cowling (loc. cit.). Using these integrals and Eucken's relation they calculated thermal conductivities of gases. However, their results were not satisfactory except for simple molecules like helium.

Franck[13] made a number of conductivity measurements in a hot-wire cell at temperatures from 100°K to 800°K, and then used these to calculate f ratios. He also split the energy terms into their component parts and after tabulating the results discussed their trends qualitatively. He found that for non-polar gases f increased with temperature to an apparent maximum and then decreased again. However, there were a number of exceptions to this.

Independently, Bromley[4] also split the energy terms into their components, and then proceeded to evaluate the coefficients of each term based on available data. The form of his equations allows conductivity to be predicted readily if viscosity and heat capacity

are available or can be estimated. Furthermore, he rendered the treatment of polar gases more amenable to engineering calculation. In a more recent paper[5] Bromley modifies his equations somewhat in view of new conductivity data available, and presents a useful summary of conductivities of a large number of substances at widely varying temperatures.

D. Theory of Measurement and Calculation.

1. Cell Constant.

As discussed elsewhere in this work, the high heat conductivity of the silver and the small width of the annular space relative to its length permit treatment of the cell as an infinite cylinder to a high degree of approximation.[46] Furthermore, the flat end surfaces may be treated as a pair of parallel plates. These simplifying assumptions are justified by the results obtained at low temperatures, which check the accepted values within a percent. Consequently, we may write for the heat conducted across the annular and other gas spaces.

$$q = q_{radial} + q_{end} + q_{corner}$$

$$q = \frac{2\pi Lk\Delta t}{\ln(r_2/r_1)} + \frac{\pi r^2 k\Delta t}{x} + q_{corner} \qquad (4)$$

For the dimensions used in our cell, it can be shown that the corner effect is less than 0.5%. By using a suitable average length L in the first term (=L + x/2) and an average $\underline{r}^2$ in the second term $[=(r_1^2 + r_2^2)/2]$, the corner effect is taken care of with a maximum error of about 0.3%. We have:

$$q = \frac{2\pi Lk\Delta t}{\ln(r_2/r_1)} + \frac{\pi r^2 k\Delta t}{x} \quad . \quad \text{(average L,r)} \qquad (5)$$

Or, we can write

$$q = C\ k\Delta t, \text{ where} \qquad (6)$$

$$C = C_1 + C_2 \qquad (6a)$$

$$C_1 = \frac{2\pi L}{\ln(r_2/r_1)} \qquad (6b)$$

$$C_2 = \frac{\pi r^2}{x} \qquad (6c)$$

The cell constant, C, is uniquely determined by the geometry of the cell. Cell constants are, therefore, a function of the temperature at which data are taken, and are listed in the Appendix. Using the cell constant, and knowing the heat input and temperature difference, the thermal conductivity may be calculated. The heat input q is obtained from electrical measurements of current and voltage. The temperature difference Δt is calculated from measured differences in thermocouple e.m.f.'s and plotted values of thermo-electric power (dE/dt) as a function of temperature. Although the temperature differences measured are not actually at the surfaces of the emitter and receiver, they are close enough so that a radial flow calculation indicates an error of 0.1% or less.

2. Effect of Pressure.

Measurements of pure conduction, of course, are required. At higher pressures convection becomes appreciable and must be eliminated. At low pressures and high temperatures, incomplete energy exchange between gas and wall become pronounced, and one must correct for the effect of temperature jump and accommodation. Gregory[14] deduced that for concentric cylinders, whose lengths are much greater than the annulus between them,

$$\frac{\Delta t}{q} = \frac{\ln(r_2/r_1)}{2\pi kL} + \frac{A}{P}\left(\frac{\sqrt{T_1}}{r_1} + \frac{\sqrt{T_2}}{r_2}\right) \qquad (7)$$

$$\text{where } A = \sqrt{\frac{2\pi M}{R}} \cdot \frac{1}{2\pi L} \cdot \frac{2-\alpha}{2\alpha(c_v/R + 1/2)} \qquad (8)$$

Thus, if $\Delta t/q$ is plotted against $1/P$, a linear relation is obtained in the absence of convection. The ordinate at $1/P$ extrapolated to zero gives the true conductivity k, and the slope gives the accommodation

coefficient. The presence of convection is indicated by a curvature of the plot at higher pressures, and extrapolation must ignore these points. (See Figure 18).

3. Radiation and Support Conduction.

In addition to gaseous conduction, parallel mechanisms of heat transfer in the cell are by conduction across the supports and radiation exchange between the emitter and receiver. It is desirable to minimize both effects and to correct for their presence. A simple means of doing so is to make "blank" runs at high vacua (1 micron Hg or better). At these low pressures the residual gas conductivity (molecular in nature) is negligible and the bulk of the $q/\Delta t$ measured is due to radiation and support conduction. These $q/\Delta t$ values may then be simply subtracted from those at moderate pressures to eliminate the effects of radiation and support conduction. It is recognized, however, that the presence or absence of gas affects the amount of support conduction. (See "Discussion".)

E. Gas Mixtures.

It was not originally intended to deal with conductivities of gas mixtures in this work. However since such data are lacking at high temperatures, sufficient data were taken to show what the mixture trends are as temperatures increase.

A number of investigators[9,24,31,36,63] have attempted to correlate mixture data but the correlation of Lindsay and Bromley[36] based on a modification of Sutherland's equation[55] appears to be about the most useful. These authors correlated 85 mixtures with an average deviation of 1.9%. However, the data they employed were all near room temperature. Their equation for a binary mixture is:

$$k(\text{mixture}) = \frac{k_1}{1 + A_{12}\, x_2/x_1} + \frac{k_2}{1 + A_{21}\, x_1/x_2} \tag{9}$$

where

$$A_{12} = 1/4 \left\{ 1 + \left[\frac{\eta_1}{\eta_2} \left(\frac{M_2}{M_1} \right)^{3/4} \frac{(1 + S_1/T)}{(1 + S_2/T)} \right]^{1/2} \right\}^2 \frac{(1 + S_{12}/T)}{(1 + S_1/T)} \tag{10}$$

A_{21} is obtained by interchanging the subscripts.

II. EXPERIMENTAL

A. Equipment.

1. Silver Cell.

The heart of the equipment is a pair of concentric silver cylinders 7" long (Figure 1). This metal was chosen because of its low emissivity and high thermal conductivity. The former property results in small radiation corrections which normally become quite significant at the high temperatures used in our experiments. The high conductivity of silver is important in order that the gas annulus may be treated as one of infinite length, symmetrical radially and isothermal axially. Because of the mass and high conductivity of the silver cylinders, virtually no temperature gradient is detectable along its length. The annular space between the cylinders is about 0.025" (0.033" in later runs). This close spacing minimizes convection and is particularly valuable in reducing the percentage radiation correction by increasing the gaseous conduction alone.

The annular symmetry is kept by means of six Lava* spacers symmetrically placed and of small dimensions so as to minimize conduction through them. These spacers contact the inner cylinder (hereafter called "emitter") at room temperature, but not all do so at elevated temperatures because of the differential expansion between silver and Lava. However, they maintain concentricity even at 800°C to within 0.002", which is sufficient to keep the error due to eccentricity to less than 0.3%. (See discussion of error, below).

---

*Product of American Lava Corporation (Chattanooga, Tennessee). Lava is a natural stone which may be machined, then fired to harden to a refractory.

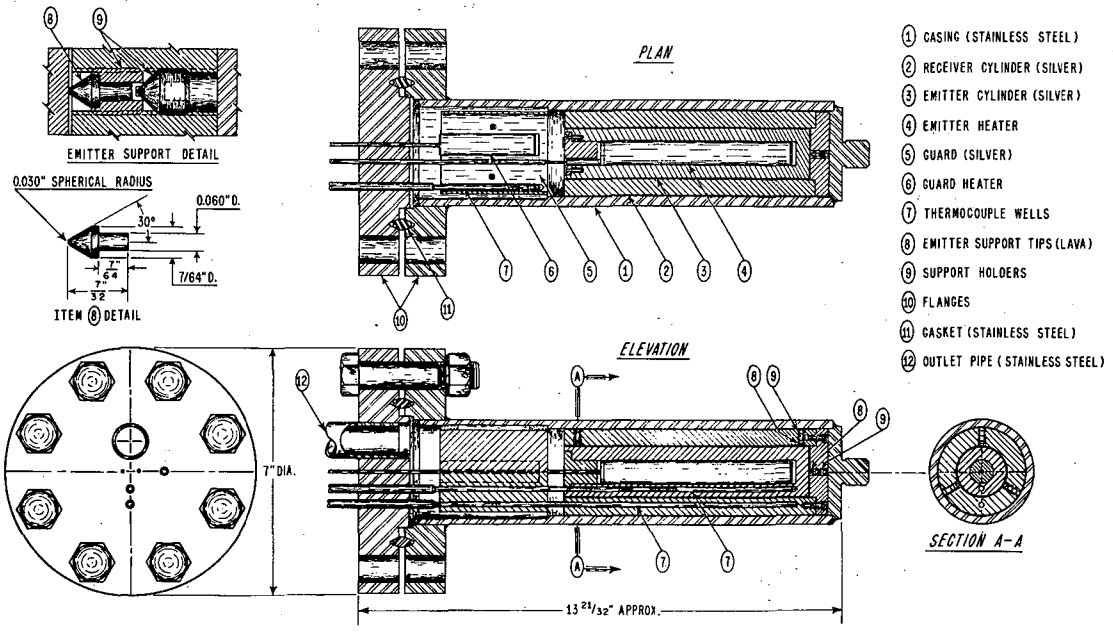

THERMAL CONDUCTIVITY CELL ASSEMBLY.

MU-6155

Figure 1

The spacers contact small (1/16" diameter) stainless steel inserts (not shown in Figure 1) in the emitter to prevent deformation of the soft silver at high temperatures.

The emitter, a solid silver piece about 1.45" in diameter, contains a 0.016" diameter nichrome wire heater in a shell of thin gauge (0.015") stainless steel. The heater in turn has short leads of 0.015" diameter platinum which are fused to 0.015" diameter gold leads 24" long. The platinum wire reduces the temperature of the leads leaving the emitter and the gold is used to minimize the voltage drop along the long leads between the emitter and the external measuring circuit. The outer cylinder (receiver) is 1.50" inside diameter and 2.5" outside diameter. Both inner and outer cylinders contain holes for thermocouple wells. These and all other silver parts were stress relieved at 300°C before machining.

At the bottom of the receiver, a solid silver disc is fastened which acts with the lower end of the emitter as a pair of parallel plates. Here, too, the emitter is supported by a Lava tip.

About 1/2" above the emitter is a "heat guard", so called because its purpose is to prevent heat flow axially upward. It has its own thermocouple well and nichrome heater so that it can be maintained at the temperature of the emitter.

These contents are all contained within a lower stainless steel casing which is flanged and bolted to a matching upper flange. The various heater and thermocouple tubes as well as an outlet pipe, are welded to the upper flange. Vacuum tightness is insured by the use of a stainless steel gasket compressed between the flanges.

2. Furnace.

The cell is placed in the center of a furnace (Figure 2) especially designed to keep a constant temperature. The center of the

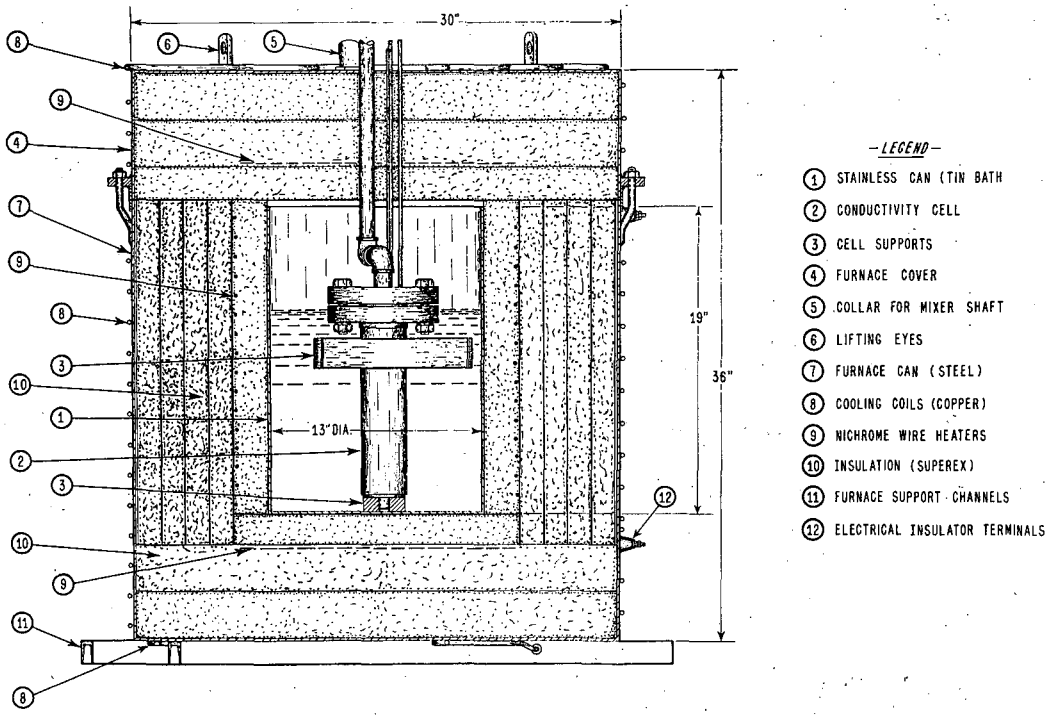

CONSTANT TEMPERATURE FURNACE.

MU-6199

Figure 2

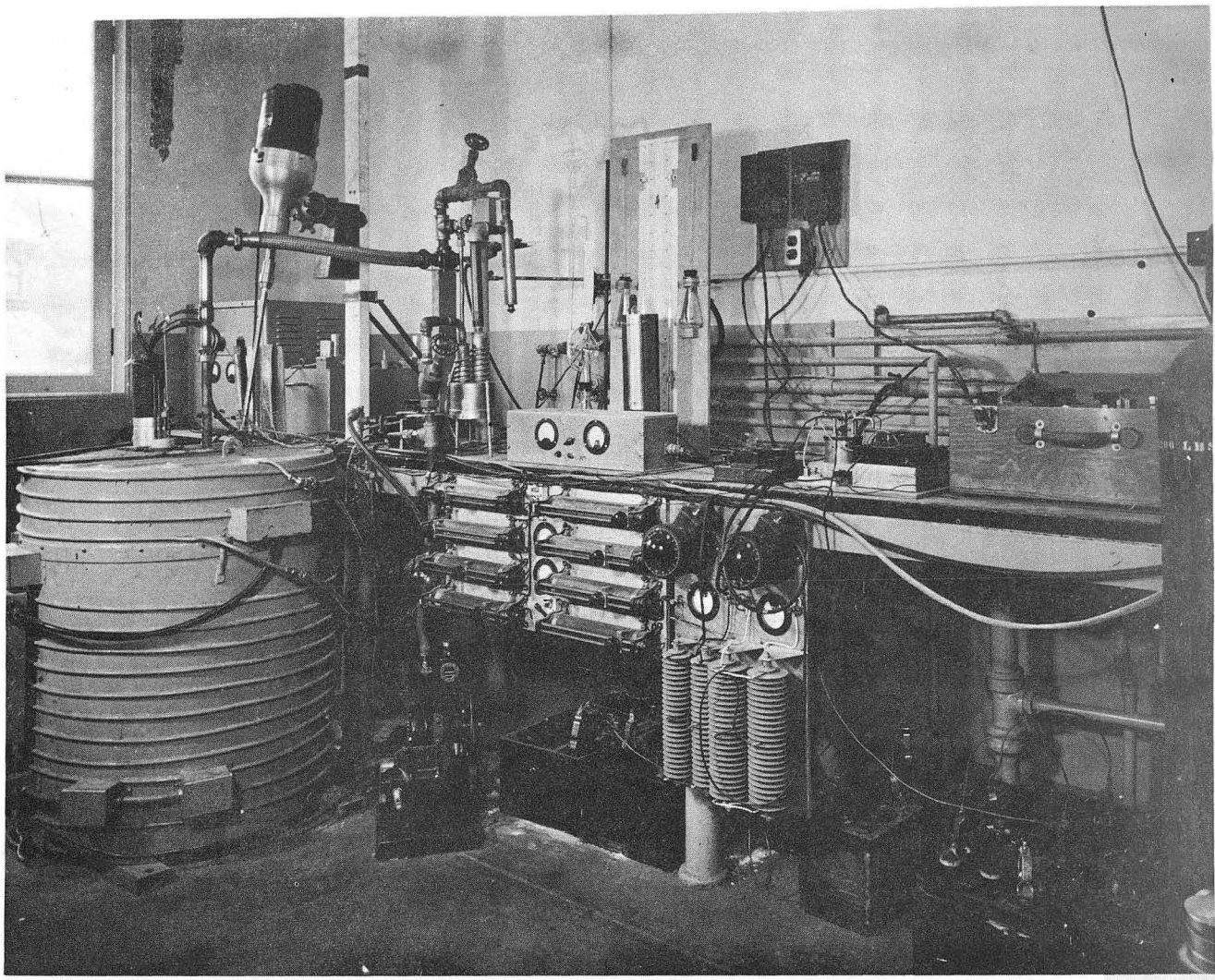

Figure 3a Photograph of Equipment

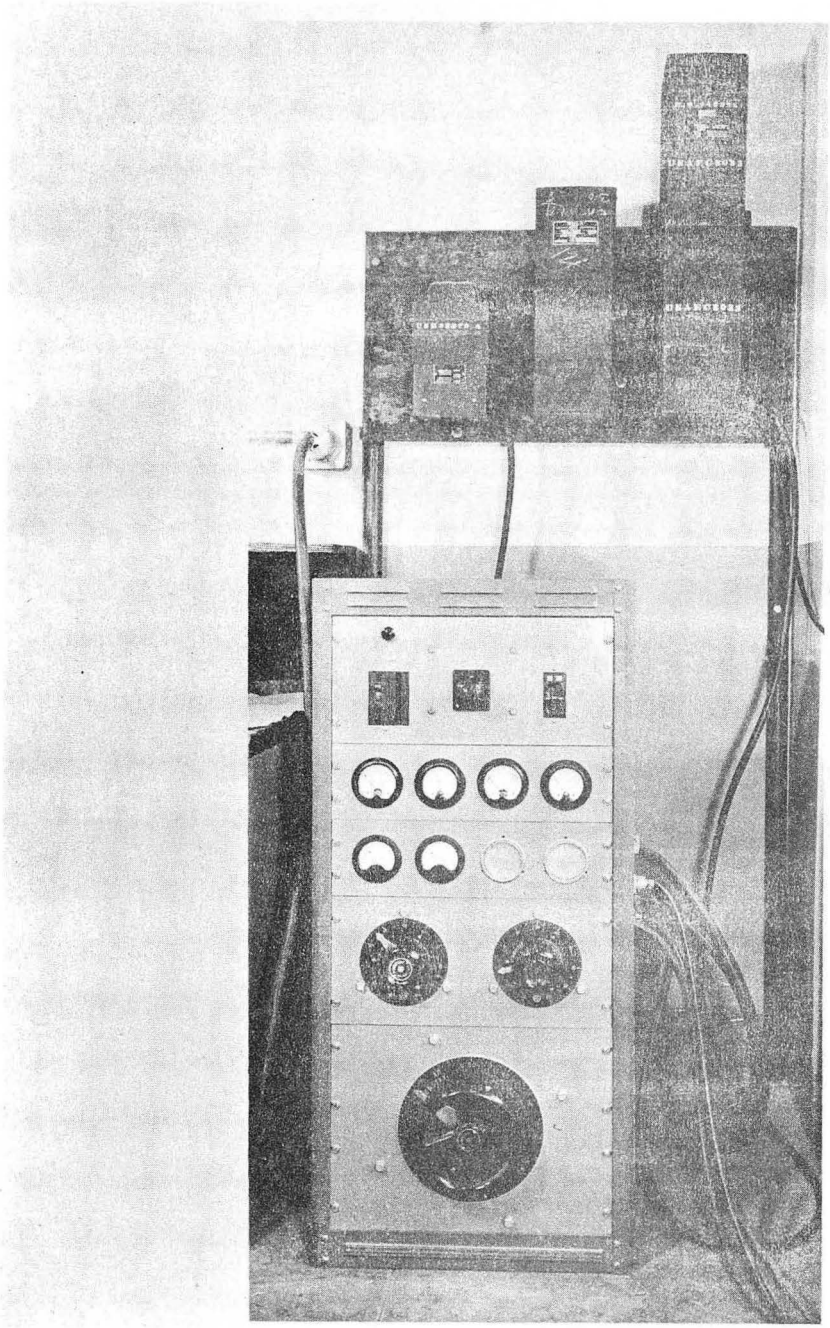

ZN-706

Figure 3b Photograph of Equipment

furnace consists of a 13" diameter stainless steel can, filled with molten tin (or water for room temperature runs). Tin was chosen because of its good thermal conductivity, low melting point (232°C), and its relative safety (non-combustibility as compared with heat transfer salts, and low toxicity[37] as compared with lead and other low-melting metals). Stainless steel was chosen as the most practicable material to withstand corrosion by tin, based on available information.[29,37] Carbon steel oxidizes rapidly at the temperature of the furnace and probably offers lower corrosion resistance to tin. Stainless walls in contact with the tin were made heavy enough to permit a degree of corrosion and still protect the equipment. A Lightnin' mixer is provided to agitate the liquid to aid in the maintenance of uniform temperature. The can is surrounded by a two-inch thickness of Johns-Manville Superex, a form of diatomaceous earth. This high temperature insulation (claimed to withstand 1900°F) was chosen because of its low thermal conductivity and thermal diffusivity, since it tends to filter out short-term temperature fluctuations in the furnace windings caused by current fluctuations before they reach the inner bath. Nichrome V coils are imbedded 1/2" into this layer at the top, center, and bottom of the furnace, each section independently controlled. Successive turns are spaced about 1/2" apart. The coils are backed by another 6" Superex layer which in turn is held in a sheet iron container. Copper cooling water coils are soldered to this casing and serve to keep it at a constant and moderate temperature. The furnace interior is accessible by means of a lid opening at the top of the furnace. Electrical circuits for the furnace are shown in Figure 4. Two basic input circuits are provided: one 8 kilowatt arrangement taken directly from house current (115 and 230 volts A.C.) for rapidly heating up the furnace, and one 3 kilowatt circuit fed

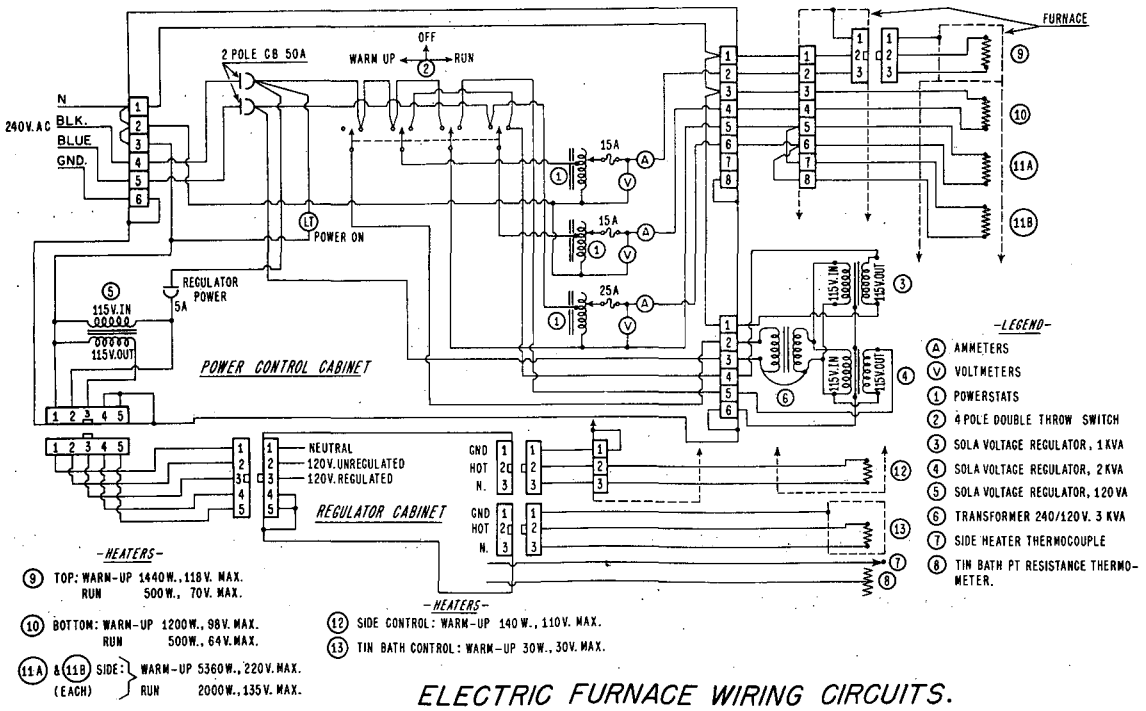
FURNACE
OFF
WARM UP
RUN
2 POLE CB 50A
N
240V.AC BLK.
BLUE
GND.
15A
15A
25A
POWER ON
REGULATOR POWER
5A
115V.IN
115V.OUT
POWER CONTROL CABINET
NEUTRAL
120V.UNREGULATED
120V.REGULATED
REGULATOR CABINET
GND
HOT
N.
-HEATERS-
9 TOP: WARM-UP 1440W., 118V. MAX.
RUN 500W., 70V. MAX.
10 BOTTOM: WARM-UP 1200W., 98V. MAX.
RUN 500W., 64V. MAX.
11A & 11B SIDE: WARM-UP 5360W., 220V. MAX.
(EACH) RUN 2000W., 135V. MAX.
-HEATERS-
12 SIDE CONTROL: WARM-UP 140W., 110V. MAX.
13 TIN BATH CONTROL: WARM-UP 30W., 30V. MAX.
-LEGEND-
A AMMETERS
V VOLTMETERS
1 POWERSTATS
2 4 POLE DOUBLE THROW SWITCH
3 SOLA VOLTAGE REGULATOR, 1 KVA
4 SOLA VOLTAGE REGULATOR, 2 KVA
5 SOLA VOLTAGE REGULATOR, 120 VA
6 TRANSFORMER 240/120V. 3 KVA
7 SIDE HEATER THERMOCOUPLE
8 TIN BATH PT RESISTANCE THERMOMETER.
ELECTRIC FURNACE WIRING CIRCUITS.
MU-6162

Figure 4

from Sola voltage regulators which keep voltage fluctuations to ± 1%. The latter circuit is used during steady state operation.

3. Temperature Controls.

The original plan of investigation called for measuring temperature differences of the order of one degree Centigrade, and so required constancy of the bath temperature to about 0.01°C. Because of the high temperature at which measurements were to be made, elaborate precautions were taken to obtain this constancy of temperature. Thus, in addition to voltage control of the windings, and the isolation of these windings from the tin bath by 2" of low conductivity insulation, two stages of automatic control were provided (Figures 5, 6, 7). One stage measures the temperature at the main windings by means of a 0.025" diam. chromel-alumel thermocouple and controls the current input to a 75 watt auxiliary heater which parallels the main windings. The other stage measures the temperature of the central bath by means of a resistance thermometer and operates a 30 watt heater immersed in the bath to keep the measured temperature to ±0.01°C. This resistance thermometer (Figure 8) consists of about 13 feet of fine (0.002" diameter) platinum wire wrapped non-inductively around a fused quartz tube in which double threaded grooves are ground. A platinum lead wire 0.008" in diameter is fused to each end of the fine wire and 24 inch long gold wire leads (0.015" diam.) in turn are welded to each platinum lead. Another pair of gold leads, joined at the ends, parallel the other leads. They serve to compensate for fluctuating temperatures to which the main leads are exposed. The whole unit is surrounded by a fused quartz covering, and the lead wires emerge from the top sealed into the tube with Araldite cement. To broaden the range of bath temperature control, a second manually-controlled bath heater of about 300 watts is provided, which can be used to change

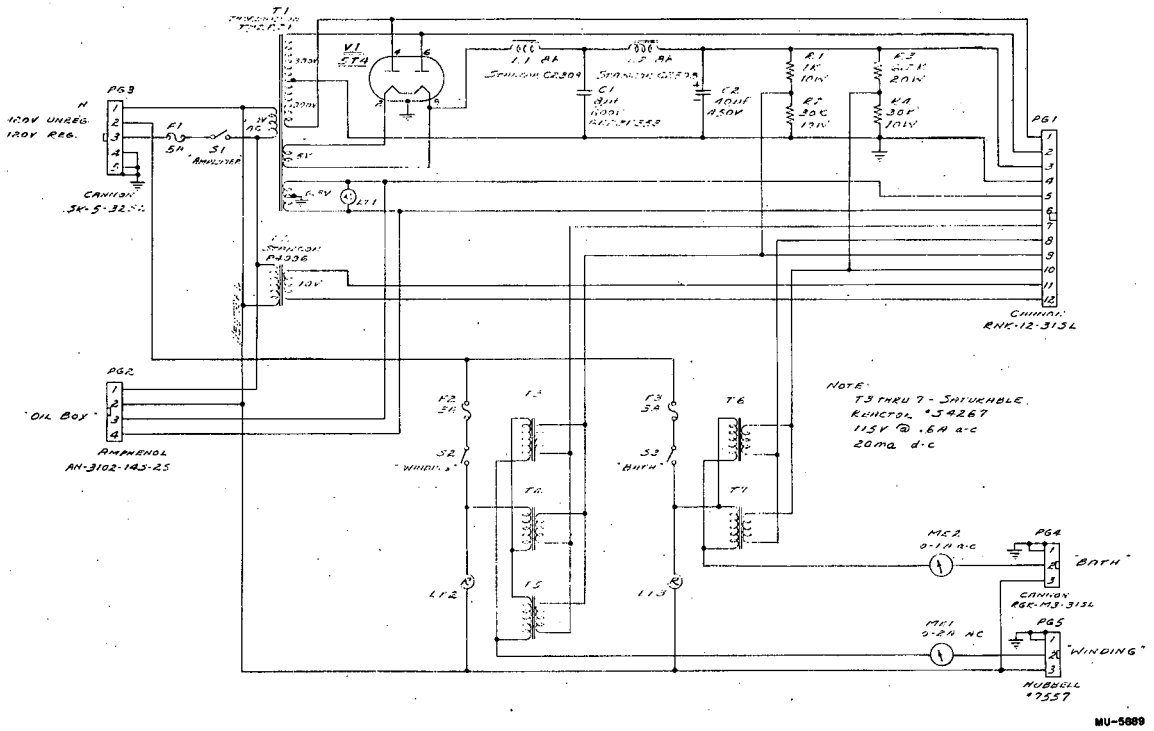

Figure 5 Temperature Controller, Power Supply

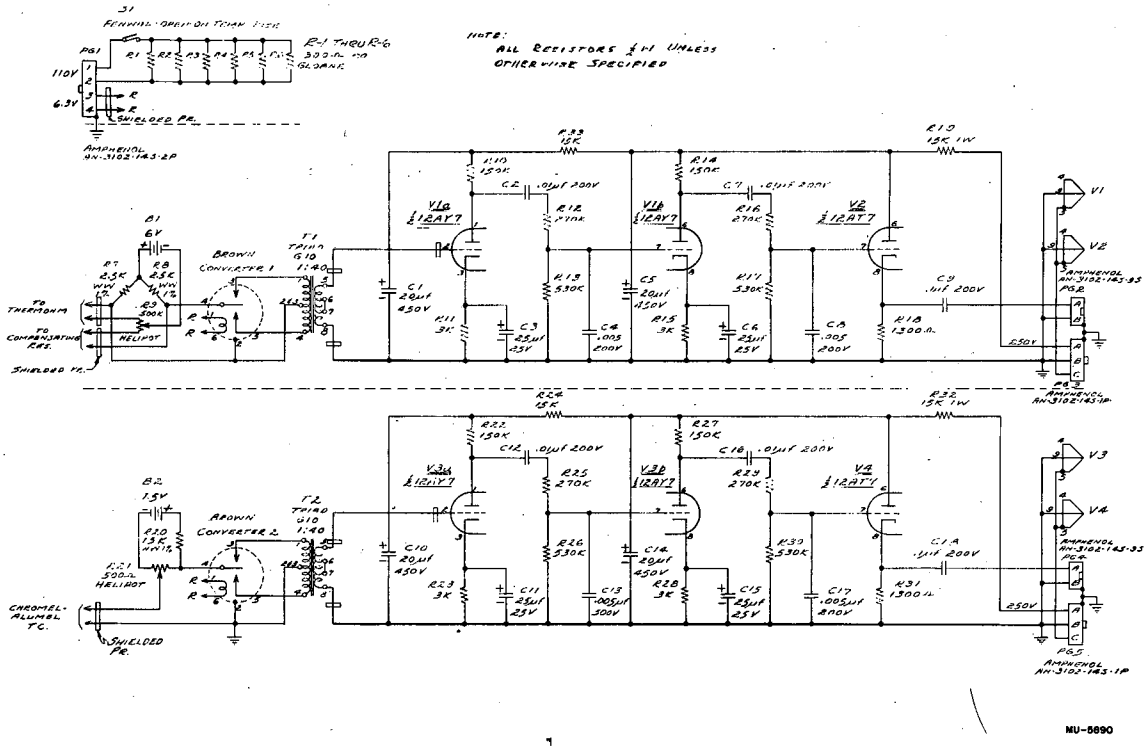

Figure 6 Temperature Controller, Pre-amplifier

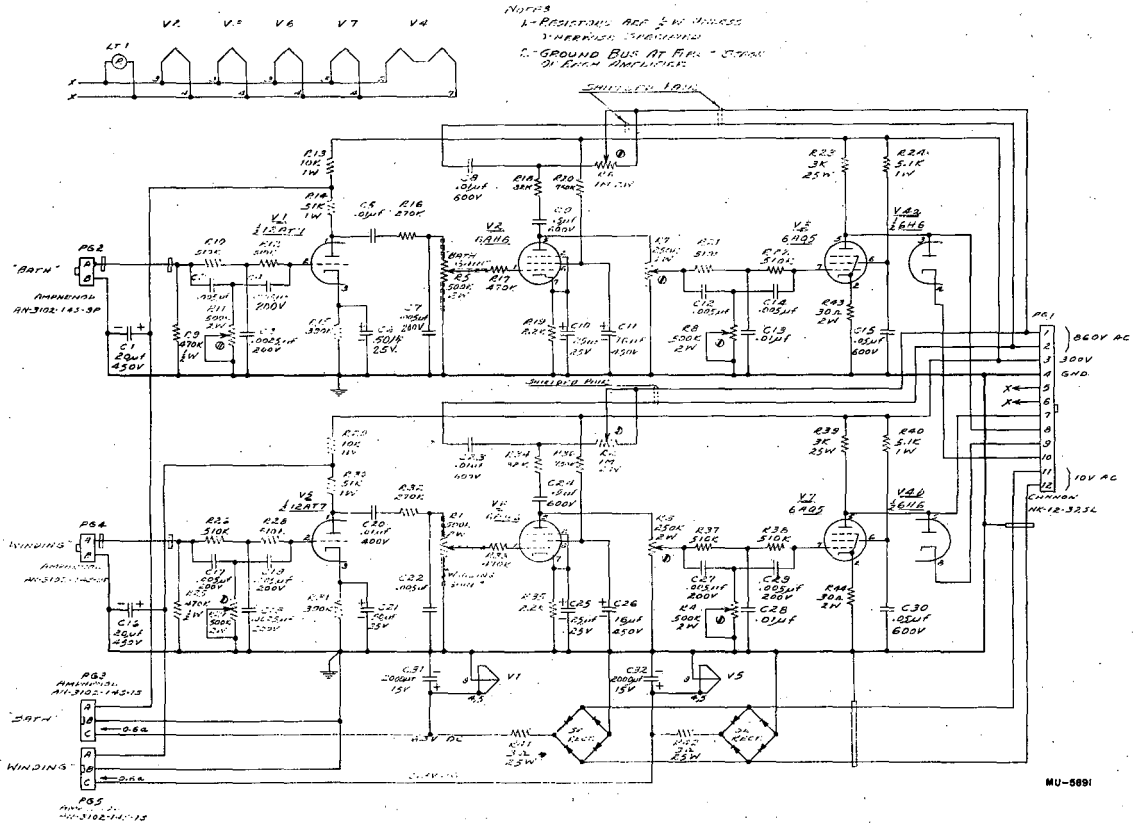

Figure 7 Temperature Controller, Amplifier

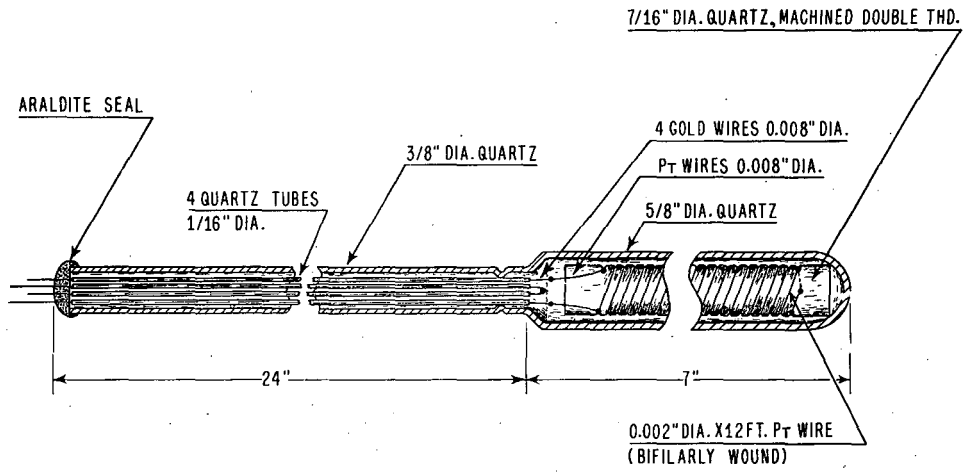

PLATINUM RESISTANCE THERMOMETER.

MU-6205

Figure 8

the temperature level by several degress to 50°C rapidly without waiting for the slow effects of the main windings. In practice it was found that the first stage of automatic control was in fact unnecessary, and so it was not used, the second stage taking over the burden of control.

The desired degree of temperature control was achieved. For periods of several hours the cell and bath temperatures remained constant to ± 0.01°C. The actual geometric uniformity of the bath temperature was not investigated carefully since the time-wise and length-wise temperature constancy within the silver cell met the requirement of ± 0.01°C. However, when the resistance thermometer and test thermocouple were moved within a space of several inches, the observed temperature remained within ± 0.01°C. This fact and the high conductivity and good stirring leads one to believe that the spatial temperature uniformity was probably within five hundredths of a degree.

4. Loading and Evacuation System.

A 3/4" I.P.S. stainless steel pipe (1" inside diameter) welded to the flange of the conductivity cell connects it to the vacuum piping (Figure 9). A Welch Duo-Seal No. 1405 vacuum pump is the forepump for a VMF-20 Distillation Products oil diffusion pump, which provides the low pressure required. Pressure measuring devices used are a McLeod Gauge (down to 0.03 microns) and thermocouple gauge (down to about 1-5 microns).

An alternate piping path is connected through a pair of magnesium perchlorate drying tubes to the required gas cylinders. An absolute mercury manometer and open-end mercury manometers for pressure and vacuum are in this branch of the circuit, as well as a pair of rotameters for metering gas mixtures.

Stainless steel is used as the piping material in the gas loading circuit, except for the vacuum shut-off valves alone (brass bellows-type), since it is envisioned that corrosive gases will eventually be

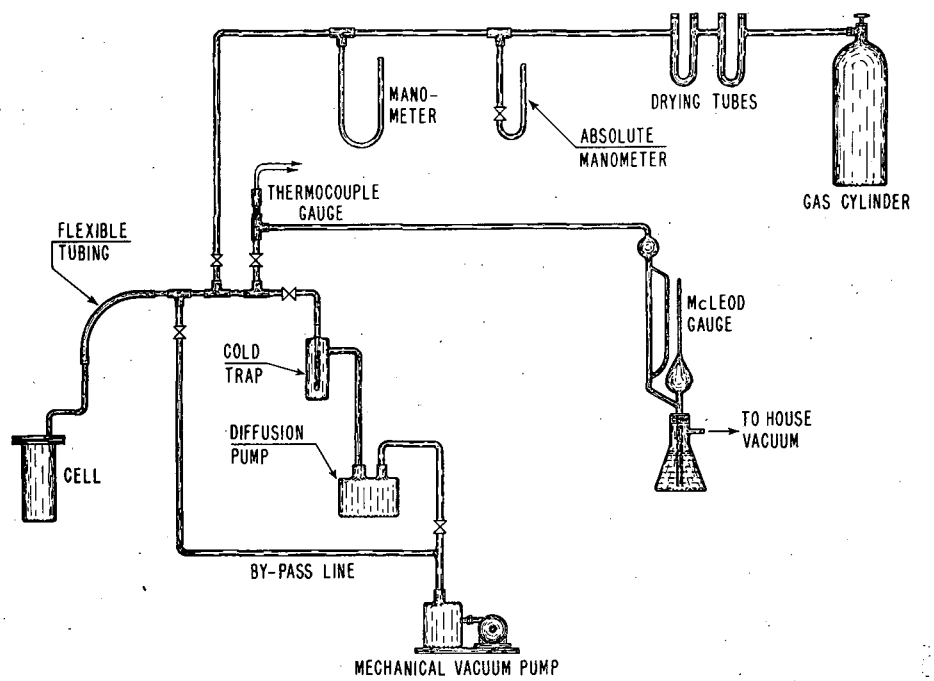

FLOW SYSTEM SCHEMATIC.

MU-6207

Figure 9

employed. For the relatively inert gases used in these experiments, clean copper connection tubes are used between the gas cylinders and the permanent piping. The vacuum piping and valves are iron and brass.

5. Cell Heating Circuits.

To provide stable heating current for both the guard and emitter, a series of from one to seven storage batteries and a source of rectified D. C. are used in parallel for each heater. By means of variable transformers (Variacs), the current through the storage batteries is adjusted to read at or slightly above zero. In this manner, the batteries are "floating" and act as a reservoir to keep the current through the heaters constant. The currents through the two heater circuits are varied roughly by varying the number of storage batteries in series, and more closely by a series of wire-wound rheostats ranging from one to 800 ohms. The emitter and guard heater resistances are respectively about 90 and 35 ohms.

In operation, the current through the emitter heater (Figure 10) is obtained by measuring the voltage drop across a standard 0.1 ohm resistor using a Leeds and Northrup No. 8662 portable potentiometer. The voltage across the heater and standard resistor together is obtained by placing a Leeds and Northrup high resistance box in parallel with them and measuring the voltage drop across a small part of the resistance (e.g. 10 ohms out of 7010 ohms total resistance). A correction (0.1%) is applied for the voltage drop in the 0.1 ohm resistor. The resistances in the box were calibrated against standard resistors and found to be correct to better than 0.1%.

6. Temperature Measurement.

The emitter, receiver, and guard are provided with wells in which the hot junctions of thermocouples are inserted. At 50°C and at some runs at 350°C, chromel-alumel couples were used, while in

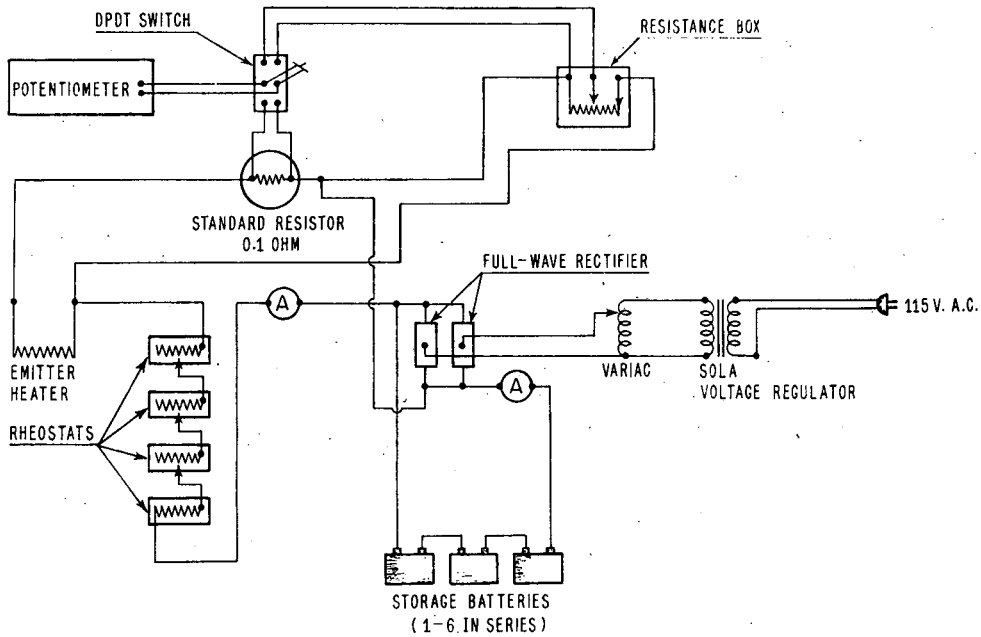

EMITTER HEATING & MEASURING CIRCUIT.

MU-6156

Figure 10

most runs at 350°C and in all above that temperature, platinum-platinum-10% rhodium couples were used. The latter are less sensitive but more stable in practice. The chromel couples (0.025" diam. wire) are threaded through two-hole refractory porcelain insulators which are inserted directly into the thermowells. The platinum couples (0.020" diam. wire) are similarly placed in insulators, which in turn are surrounded by refractory porcelain protecting tubes to prevent contamination of the platinum. These tubes are set into the wells. Couples were calibrated as described in a later section.

The cold junctions are placed in a thermos containing distilled water and finely crushed, well-packed ice. Copper leads run from the ice bath to the White double potentiometer. This potentiometer has a 10,000 microvolt range and has a smallest dial division of 1 microvolt. Fractions of a microvolt are obtained by deflection readings of a Leeds and Northrup No. 2285-b high sensitivity galvanometer. The sensitivity of the galvanometer and scale as used is about 0.05 to 0.07 microvolts per millimeter scale deflection. The entire measuring system is kept at the same potential by interconnected shields. Thermocouples are connected to the potentiometer to read the following temperatures:

1. Temperature of the receiver or emitter (on the "P" scale of the White)

2. Temperature difference between emitter and receiver (on the "Q" scale)

3. Temperature difference between emitter and guard (on the "D" or deflection scale).

B. Procedure.

1. Gas Measurements.

The furnace is heated up to the required temperature (usually overnight) and then the controls are set by trial and error for the desired temperature level. Heating current for the guard and emitter is turned on, and the storage battery current adjusted to zero so the batteries are "float" charging, or behaving as energy reservoirs to filter out variations in the heating current. In this manner the current remains steady to between 0.1 and 0.01% for several hours at a time. The cell is thoroughly evacuated by means of the mechanical pump, and the desired gas is allowed to flow in. The cell and its piping are purged several times to clear them of air or other impurities, and then the cell is filled with the gas and equalized to atmospheric pressure. Then temperature readings are taken periodically by means of the White potentiometer, until the receiver and emitter temperatures remain constant for several successive 10-minute periods. The guard heater current is adjusted while steady state is approached so that the guard and emitter temperatures are kept the same (within a few hundredths of a degree). Periodically, emitter heater current and voltage measurements are recorded.

All couples were annealed before calibration. The chromel couples were heated in air at 650°C for 48 hours, while the platinum couples were heated in air at 1450°C for one hour, a procedure recommended by the Bureau of Standards.[45] One thermocouple of each type was calibrated by the Bureau of Standards, the chromel-alumel couple at 100°C intervals from zero to 500°C and the platinum-rhodium couple from zero to 1000°C at 50°C intervals. A smooth curve of dE/dt vs. temperature (Figure 25) was obtained for the latter, after plotting differences in e.m.f.'s for two successive temperatures divided by

the difference between these temperatures. The chromel couple, on the other hand, showed typical humps in the region of 0°-200°C. To obtain the dE/dt more precisely for the chromel couples in the region 0 to 50°C, their hot junctions were taped around a glass thermometer which had been calibrated by the Bureau of Standards. The assembly was then placed in a covered one gallon dewar filled with water and a powerful stirrer used to circulate the water. Simultaneous readings of the thermometer and thermocouples were taken and from these values dE/dt plots were made. (See Appendix). Results were reproducible.

Intercalibration of the thermocouples was carried out at each temperature and checked several times a day during the early runs and once or twice a week in the later runs. To accomplish this, a set of steady-state readings were made, and then the couples were quickly removed from their tubes and interchanged. Again readings were taken. Finally, the couples were returned to their original locations to check the result. In this manner corrections to each couple were made so that its e.m.f. could be known in terms of the standard couple. The guard couple was also interchanged with one of the other couples to obtain its correction at each temperature. For the platinum couples the corrections ranged from about 2 microvolts at 350°C to about 8 microvolts at 780°C between the emitter and receiver couples and from about 12 to 18 microvolts at the same temperature extremes between the emitter and guard couples. The various chromel couples differed by zero to 20 microvolts at 50°C and by 50 to 80 microvolts at 350°C.

2. Gas Mixtures.

Gas mixture runs are made by passing the gases from their cylinders through intercalibrated rotameters to a single six-foot section of 3/16" diameter tube where the gases mix while flowing. The mixture flows to atmosphere while the cell is being evacuated,

and then a small part of the mixture is gradually bled into the evacuated cell while the bulk of it still flows to atmosphere. In this way the rotameter bobs are stable since the back pressure remains constant at slightly over one atmosphere. After filling the cell, the procedure followed is identical with that used for pure gases.

3. High Vacuum Runs.

In order to correct for net radiation between the silver emitter and receiver, and for conduction across the solid supports, runs are made at high vacua (about 10^{-4} mm Hg). These are carried out in a manner similar to that for the gas runs, except that considerably longer times are required to reach equilibrium (several hours at high temperatures to several days at room temperature). The method of applying the correction is discussed below.

4. Pressure Runs.

To correct for convection and accommodation-temperature jump effects, series of runs are made at varying pressures. These are carried out as described above for ordinary gas runs, except that after steady state is reached at a pressure of one or several atmospheres, the gas is partially evacuated to the new desired pressure. Readings are again taken until a new steady state is reached, and the process repeated. Occasionally between successive pressure runs and usually at the end of a pressure series, the system is evacuated and flushed with fresh gas and measurements are made to check the earlier atmospheric pressure result. The application and significance of the pressure runs are discussed in a later section.

III. RESULTS

Gases measured were nitrogen, carbon dioxide, air, argon, helium, and mixtures of nitrogen and carbon dioxide. The observed and calculated results are listed in Tables I, II and III. The tabular values of thermal conductivity at one atmosphere have been corrected for radiation and convection as discussed elsewhere in this paper. In addition, plots of thermal conductivity versus temperature have been made, as well as comparisons between our values and those of other investigators (Figures 11-16). Two types of conductivity plots are presented for nitrogen and carbon dioxide. One plot for each indicates as dots all the data measured, to give some idea of the maximum scatter. These plotted points were then grouped according to temperature level. The range of values clustering about a particular level was small (12°C maximum), so that negligible error was introduced by adjusting these data to a common temperature by means of the slope of conductivity vs. temperature at that point. The data of each group were then averaged, and the average value indicated on the second plot. Points known to be in error (see "Discussion") were not included in the second plot. This latter plot also includes conductivity values obtained by some recent investigators, for comparison with ours.

Graphical plots of vacuum runs ($q/\Delta t$ vs. T^3), and representative "pressure-effect" runs ($\Delta t/q$ vs. $1/P$) are given (Figures 17 and 18). Their interpretation is considered in the "Discussion".

Conductivities of nitrogen-carbon dioxide mixtures are plotted as functions of composition at various temperatures (Figures 19 and 20). The Lindsay-Bromley correlation[36] is also plotted for comparison at each temperature level.

The cell designations 1A, 1B, 1C, 2A and 2B in Table I refer to particular assemblies of the cell. Each time the cell was put together

after dismantling, the next successive letter designation was used. These assemblies differed merely in bottom spacing. Number 2 was applied after the silver cylinders were remachined, and so its annular spacing differs from that of Cell No. 1. For the cell constants and relevant dimensions of each cell, see Tables VI and VII in the Appendix.

Table I.

Experimental Data

Run	Cell	Gas	Press. Hg.	$t_{av.}$ °C	Δt °C	q watts	Vac. Corr'n. watts/°C	q/Δt* watts/°C	k x 10^5 cal./sec.°C cm.
1	1A	Air	760 mm	41	7.19	6.616	0.003	0.917	6.43
2			760	32	0.833	0.7477	0.003	0.895	6.27
3			760	34	0.810	0.7507	0.003	0.924	6.48
4			760	36	3.20	2.890	0.003	0.900	6.31
5			760	44	12.26	11.51	0.003	0.936	6.56
6A		Vac.	3.5 μ	28	4.38	0.0212	-	0.0048	
6B		Vac.	4 u	27	4.64	0.0220	-	0.0047	
7	1B	Air	760 mm	46	5.75	5.301	0.004	0.918	6.46
9		Vac.	7.5 μ	51	4.42	0.0535	-	0.012	
10A		Air	760	52	3.67	3.456	0.004	0.938	6.60
10B			413	52	3.71	3.456	0.004	0.928	
10C			168	52	3.69	3.456	0.004	0.933	
10D			78	52	3.65	3.456	0.004	0.943	
10E			45	52	3.66	3.446	0.004	0.938	
10F			760	52	3.70	3.446	0.004	0.927	6.52
10G			25	52	3.70	3.446	0.004	0.927	
10H			15	52	3.71	3.446	0.004	0.925	
10K			3.3	52	4.79	3.448	0.004	0.716	
11			760	56	7.14	6.810	0.004	0.950	6.69
12		N_2	760	56	7.24	6.804	0.004	0.936	6.59
13		N_2	760	53	3.41	3.136	0.004	0.917	6.46
14		Argon	760	54	4.92	3.198	0.004	0.646	4.55
15A		Air	760	55	9.14	8.619	0.004	0.939	6.61
15B			24	55	9.22	8.613	0.004	0.930	
15C			17.5	55	9.19	8.613	0.004	0.933	
15D			13.5	55	9.19	8.613	0.004	0.933	
15E			760	55	9.14	8.592	0.004	0.936	6.59
15F			22.8	55	9.11	8.592	0.004	0.940	
16		N_2	760	368	11.80	19.50	0.033	1.620	11.26
17			760	362	2.98	4.832	0.033	1.591	11.06
18			760	361	2.96	4.855	0.033	1.608	11.17
19			760	361	2.79	4.828	0.033	1.696	11.78
20			760	362	6.38	10.29	0.033	1.579	10.97
21			756	366	12.15	20.01	0.032	1.615	11.23
22A			756	366	12.58	20.21	0.032	1.575	10.95
22B			410	366	12.60	20.21	0.032	1.572	
22C			274	366	12.71	20.21	0.032	1.558	
22D			756	366	12.57	20.22	0.032	1.577	10.96
22E			250	366	12.71	20.23	0.032	1.560	
22F			140	366	12.79	20.23	0.032	1.550	
22G			72	366	12.89	20.23	0.032	1.537	
22H			41	366	13.01	20.23	0.032	1.523	

* including vacuum correction

Table I. (cont'd)

Run	Cell	Gas	Press. Hg.	$t_{av.}$ °C	Δt °C	q watts	Vac. Corr'n. watts/°C	g/Δt* watts/°C	k x 10^5 cal. / sec.°C cm.
22I	1B	N_2	18	367	13.24	20.24	0.032	1.497	
22J			9	367	13.61	20.24	0.032	1.455	
22K			4	368	14.19	20.24	0.032	1.394	
22L			2	372	17.35	20.24	0.033	1.134	
22M			756	366	12.65	20.29	0.032	1.572	10.93
22N		N_2	56 μ	374	19.62	2.543	0.033	0.097	
23A		Vac.	14 μ	365	12.18	0.7556	-	0.062	
23B		Vac.	8 μ	362	14.95	0.7556	-	0.051	
24A		N_2	755 mm	355	3.28	5.028	0.030	1.503	10.45
24B		N_2	255	355	3.29	5.023	0.030	1.497	
24C			140	355	3.31	5.023	0.030	1.488	
24D			752	355	3.28	5.023	0.030	1.501	10.44
24E			140	355	3.31	5.019	0.030	1.487	
24F			70	355	3.35	5.016	0.030	1.467	
24G			35	355	3.40	5.016	0.030	1.445	
24H			16	355	3.50	5.014	0.030	1.403	
24I			7	356	3.73	5.014	0.030	1.314	
26		Vac.	0.4 μ	376	13.22	0.4414	-	0.033	
27		Vac.	0.4 μ	374	7.17	0.2451	-	0.034	
28		CO_2	755 mm	376	12.24	18.54	0.033	1.482	10.30
29			755	377	6.03	9.114	0.033	1.478	10.27
30			755	375	1.92	2.860	0.033	1.457	10.13
31			755	378	6.29	9.414	0.033	1.465	10.18
31A			755	378	6.34	9.410	0.033	1.452	10.09
31B			290	378	6.14	9.374	0.033	1.493	
31C			141	378	6.13	9.368	0.033	1.495	
31D			70	378	6.16	9.356	0.033	1.485	
31E			750	378	6.32	9.356	0.033	1.447	10.06
33		N_2	753	378	5.77	9.353	0.033	1.588	11.04
34		CO_2	755	358	6.30	9.384	0.033	1.456	10.13
37			755	358	6.33	9.384	0.031	1.451	10.09
38		N_2	755	358	5.87	9.384	0.031	1.568	10.90
42		CO_2	755	358	6.38	9.412	0.031	1.445	10.04
43		Argon	758	360	8.45	9.430	0.032	1.084	7.54
44		Argon	758	558	6.78	9.326	0.077	1.298	8.98
45		N_2	758	557	4.77	9.329	0.077	1.878	12.99
48		CO_2	758	557	4.68	9.187	0.078	1.887	13.05
51		N_2	761	557	4.66	9.225	0.077	1.902	13.17
52		CO_2	763	557	4.70	9.225	0.077	1.885	13.04
53	1C	Vac.	0.1 μ	382	27.28	0.9686	-	0.035	
54		N_2	756 mm	369	7.24	11.68	0.033	1.581	11.02
55		CO_2	756	369	7.67	11.69	0.033	1.491	10.40
60		25% CO_2 75% N_2	756	369	7.26	11.71	0.033	1.581	11.02

* including vacuum correction

Table I. (cont'd)

Run	Cell	Gas	Press. Hg.	$t_{av.}$ °C	Δt °C	q watts	Vac. Corr'n. watts/°C	q/Δt* watts/°C	k x 10^5 cal. / sec.°C cm.
61	1C	47% CO_2 53% N_2	767 mm	369	7.34	11.71	0.033	1.563	10.91
62		N_2	756	369	7.18	11.72	0.033	1.600	11.16
63		N_2	756	369	7.19	11.68	0.033	1.592	11.09
64		50% CO_2 50% N_2	756	369	7.23	11.68	0.033	1.583	11.03
64A		50% CO_2 50% N_2	756	369	7.33	11.68	0.033	1.560	10.88
65		CO_2	756	370	7.62	11.68	0.033	1.501	10.46
66		N_2	756	369	6.99	11.52	0.033	1.614	11.25
67		50% CO_2 50% N_2	756	369	7.18	11.52	0.033	1.572	10.96
67A		50% CO_2 50% N_2	756	369	7.17	11.52	0.033	1.575	10.97
68		50% CO_2 50% N_2	756	369	7.20	11.52	0.033	1.568	10.93
69		CO_2	756	369	7.55	11.50	0.033	1.489	10.39
70		50% CO_2 50% N_2	756	369	7.22	11.53	0.033	1.564	10.92
71		N_2	756	369	6.98	11.53	0.033	1.618	11.28
72		N_2	756	369	2.34	3.833	0.033	1.604	11.18
73		N_2	756	472	6.24	11.39	0.054	1.772	12.32
74		CO_2	756	472	6.33	11.39	0.054	1.746	12.15
75		44% CO_2 56% N_2	756	471	6.14	11.40	0.054	1.804	12.56
76		N_2	756	471	6.32	11.39	0.054	1.748	12.16
77		Vac.	0.1 μ	475	12.78	0.6874	-	0.054	
78		Vac.	0.3 μ	570	7.96	0.6536	-	0.082	
79		N_2	750	569	6.34	12.50	0.082	1.891	13.14
80		50% CO_2 50% N_2	750	569	6.00	12.50	0.082	2.000	13.88
81		CO_2	750	569	6.11	12.50	0.082	1.962	13.62
82		67% CO_2 33% N_2	750	569	6.04	12.50	0.082	1.986	13.78
83		33% CO_2 67% N_2	750	569	5.98	12.50	0.082	2.008	13.94
84		N_2	750	569	6.13	12.50	0.082	1.957	13.59
85A		N_2	750	568	6.14	12.47	0.082	1.950	13.54
85B			371	569	6.25	12.48	0.082	1.915	
85C			750	569	6.14	12.48	0.082	1.951	13.54
85D			240	569	6.32	12.48	0.082	1.894	

* including vacuum correction

Table I. (cont'd)

Run	Cell	Gas	Press. Hg.	$t_{av.}$ °C	Δt °C	q watts	Vac. Corr'n. watts/°C	q/Δt* watts/°C	k x 10^5 cal./sec.°C cm.
85E	1C	N_2	130 mm	569	6.40	12.48	0.082	1.868	
85F			66	569	6.54	12.48	0.082	1.828	
85G			19	569	7.22	12.48	0.082	1.647	
85H			750	569	6.13	12.48	0.082	1.954	13.56
86			752	573	12.08	24.34	0.083	1.932	13.42
87		50% CO_2 50% N_2	752	572	11.49	24.40	0.083	2.041	14.17
88		CO_2	752	573	11.73	24.40	0.083	1.997	13.87
89		67% CO_2 33% N_2	752	573	11.60	24.40	0.083	2.020	14.03
90		33% CO_2 67% N_2	752	572	11.49	24.43	0.083	2.043	14.19
91		Argon	752	576	17.20	24.38	0.084	1.333	9.26
92A		N_2	752	573	12.16	24.40	0.083	1.923	13.35
92B			390	573	12.31	24.40	0.083	1.899	
92C			189	573	12.45	24.43	0.083	1.879	
92D			90	573	12.71	24.40	0.083	1.837	
92E			756	573	12.32	24.82	0.083	1.932	13.42
93A			750	567	3.05	5.974	0.081	1.877	13.03
93B			377	567	3.06	5.969	0.081	1.868	
93C			191	567	3.10	5.969	0.081	1.844	
93D			752	567	3.02	5.969	0.081	1.895	13.16
93E			752	567	2.97	5.955	0.081	1.924	13.36
94			752	567	2.97	5.955	0.081	1.924	13.36
95A			750	678	9.78	22.56	0.111	2.195	15.20
95B			750	678	9.77	22.43	0.111	2.184	15.12
95C			376	678	9.92	22.40	0.111	2.147	
95D			202	678	10.05	22.41	0.111	2.119	
95E			98	678	10.27	22.40	0.111	2.070	
95F			39	679	10.81	22.40	0.111	1.961	
97		50% CO_2 50% N_2	752	677	9.11	22.40	0.111	2.348	16.27
98		CO_2	752	677	9.19	22.38	0.111	2.324	16.10
99		N_2	752	688	4.85	11.29	0.114	2.215	15.34
100		25% CO_2 75% N_2	752	688	4.58	11.29	0.114	2.351	16.29
101		50% CO_2 50% N_2	752	688	4.52	11.29	0.114	2.384	16.51
102		75% CO_2 25% N_2	752	688	4.54	11.29	0.114	2.373	16.44
103		CO_2	752	688	4.60	11.29	0.114	2.340	16.21
104		Argon	752	689	6.91	11.29	0.114	1.520	10.52
105		Vac.	1.0 μ	688	8.00	0.913	.-	0.114	
106		CO_2	752	687	4.63	11.30	0.114	2.326	16.11

* including vacuum correction

Table I. (cont'd)

Run	Cell	Gas	Press. Hg.	$t_{av.}$ °C	Δt °C	q watts	Vac. Corr'n. watts/°C	q/Δt* watts/°C	k x 10^5 cal./sec.°C cm.
107A	1C	CO_2	754 mm	687	4.62	11.18	0.114	2.306	15.97
107B			1492	687	4.57	11.18	0.114	2.332	
107C			377	687	4.64	11.19	0.114	2.298	
107D			195	687	4.70	11.20	0.114	2.269	
107E			90	687	4.81	11.21	0.114	2.217	
108A		N_2	756	687	4.83	11.22	0.114	2.209	15.30
108B			1498	687	4.73	11.23	0.114	2.260	
108C			374	687	4.98	11.23	0.114	2.141	
108D			195	687	5.09	11.23	0.114	2.092	
108E			3040	687	4.74	11.28	0.114	2.266	
108F			2278	687	4.79	11.31	0.114	2.247	
108G			1516	687	4.84	11.28	0.114	2.217	
108H			756	687	4.93	11.28	0.114	2.174	15.06
110A		Argon	754	688	6.96	11.29	0.114	1.508	10.44
110B			1516	688	6.95	11.29	0.114	1.510	
110C			3042	688	6.95	11.30	0.114	1.512	
110D			374	688	6.96	11.30	0.114	1.505	
110E			185	688	7.06	11.32	0.114	1.490	
110F			50	688	7.35	11.32	0.114	1.426	
111A		Helium	754	686	2.22	23.57	0.114	10.50	77.7
111B			1516	686	2.15	23.56	0.114	10.85	
111C			3042	686	2.12	23.57	0.114	11.01	
111D			374	686	2.36	23.58	0.114	9.878	
111E			185	686	2.64	23.58	0.114	8.818	
111F			82	686	3.34	23.58	0.114	6.946	
112A		N_2	3042	690	9.73	23.57	0.115	2.307	
112B			1516	690	9.92	23.56	0.115	2.260	
112C			758	690	10.11	23.56	0.115	2.215	15.34
113A			753	775	7.05	18.19	0.163	2.417	16.71
113B			1515	774	6.89	18.18	0.163	2.475	
113C			3038	775	6.77	18.17	0.163	2.522	
113D			372	775	7.17	18.16	0.163	2.369	
113E			180	775	7.32	18.16	0.163	2.318	
113F			93	775	7.49	18.14	0.163	2.260	
113G			45	775	7.84	18.13	0.163	2.150	
114A		CO_2	753	774	6.46	18.13	0.163	2.645	18.29
114B			397	774	6.61	18.13	0.163	2.578	
114C			177	774	6.88	18.15	0.163	2.474	
115		50% CO_2 50% N_2	753	774	6.46	18.13	0.163	2.645	18.29
116A		50% CO_2 50% N_2	747	774	6.47	18.13	0.163	2.641	18.26
116B		50% CO_2 50% N_2	378	774	6.54	18.18	0.163	2.617	
116C		50% CO_2 50% N_2	177	774	6.70	18.18	0.163	2.551	

* including vacuum correction

Table I. (cont'd)

Run	Cell	Gas	Press. Hg.	$t_{av.}$ °C	Δt °C	q watts	Vac. Corr'n. watts/°C	q/Δt* watts/°C	k x 10^5 cal. / sec.°C cm.
117	1C	N_2	753mm	773	3.48	9.26	0.163	2.497	17.27
118		Vac.	1 μ	771	3.02	0.4711	.-	0.161	
119A		N_2	753	372	5.56	9.660	0.035	1.702	11.87
119B			369	372	5.64	9.647	0.035	1.675	
119C			178	372	5.73	9.641	0.035	1.648	
119D			83	372	5.85	9.641	0.035	1.613	
120		50% CO_2 50% N_2	753	372	5.68	9.656	0.035	1.665	11.61
121		33% CO_2 67% N_2	753	372	5.58	9.653	0.035	1.695	11.82
122		CO_2	756	372	5.95	9.653	0.035	1.587	11.06
123		67% CO_2 33% N_2	753	372	5.80	9.653	0.035	1.629	11.36
124		33% CO_2 67% N_2	753	372	5.58	9.656	0.035	1.695	11.82
125		N_2	755	372	5.55	9.656	0.035	1.705	11.89
126		17% CO_2 83% N_2	753	372	5.54	9.656	0.035	1.708	11.91
127		N_2	753	370	2.68	4.650	0.034	1.701	11.86
128A			754	376	10.49	18.26	0.035	1.706	11.89
128B			376	376	10.59	18.26	0.035	1.689	
128C			175	376	10.69	18.24	0.035	1.671	
128D			71	376	10.95	18.25	0.035	1.632	
128E			40	376	11.24	18.22	0.035	1.586	
128F			754	376	10.45	18.24	0.035	1.710	11.92
129		17% CO_2 83% N_2	754	376	10.27	18.24	0.035	1.741	12.14
130A		50% CO_2 50% N_2	754	375	9.11	15.72	0.035	1.691	11.79
130B		50% CO_2 50% N_2	754	375	9.06	15.61	0.035	1.688	11.77
131		33% CO_2 67% N_2	754	375	8.85	15.54	0.035	1.721	12.00
132		67% CO_2 33% N_2	754	375	9.18	15.50	0.035	1.653	11.53
133		17% CO_2 83% N_2	754	375	8.75	15.46	0.035	1.732	12.08
134		N_2	754	375	8.90	15.47	0.035	1.703	11.87
135A		CO_2	754	375	9.75	15.97	0.035	1.603	11.18
135B			380	375	9.80	15.97	0.035	1.595	
135C			175	375	9.87	15.95	0.035	1.581	
135D			80	375	9.95	15.91	0.035	1.564	
135E			41	375	10.15	15.87	0.035	1.529	
135F			1507	375	9.59	15.83	0.035	1.616	

* including vacuum correction

Table I. (concluded)

Run	Cell	Gas	Press. Hg.	$t_{av.}$ °C	Δt °C	q watts	Vac. Corr'n. watts/°C	q/Δt* watts/°C	k x 10^5 cal./sec.°C cm.
135G	1C	CO_2	3040 mm	375	9.57	15.84	0.035	1.620	
135H			754	375	9.66	15.85	0.035	1.606	11.20
136		Vac.	1.0 μ	374	11.01	0.3920	-	0.035	
137A		N_2	3050 mm	371	3.05	5.308	0.035	1.705	
137B			1510	371	3.09	5.331	0.035	1.690	
137C			760	371	3.13	5.357	0.035	1.677	11.70
137D			378	371	3.17	5.366	0.035	1.658	
137E			179	371	3.22	5.366	0.035	1.631	
137F			110	371	3.24	5.373	0.035	1.623	
137G			76	371	3.24	5.368	0.035	1.621	
137H			41	371	3.32	5.368	0.035	1.582	
137I			18	371	3.52	5.373	0.035	1.491	
138			753	371	3.12	5.345	0.035	1.678	11.71
139A		50% CO_2 50% N_2	753	371	3.18	5.350	0.035	1.647	11.49
139B		50% CO_2 50% N_2	223	371	3.21	5.352	0.035	1.632	
139C		50% CO_2 50% N_2	109	371	3.24	5.359	0.035	1.619	
139D		50% CO_2 50% N_2	53	371	3.33	5.359	0.035	1.574	
141	2A	N_2	753	366	7.60	9.50	0.032	1.219	11.17
143			753	366	7.67	9.50	0.032	1.206	11.06
144			753	371	14.10	17.69	0.033	1.222	11.20
145			753	377	25.42	32.39	0.034	1.240	11.37
146			753	669	5.89	10.37	0.107	1.654	15.06
147			751	688	5.76	10.25	0.114	1.665	15.16
148			751	688	5.79	10.33	0.114	1.671	15.21
149		CO_2	751	688	5.56	10.32	0.114	1.742	15.86
150			751	772	10.45	21.44	0.161	1.891	17.19
151		N_2	751	772	11.01	21.41	0.161	1.784	16.22
152			751	769	7.72	14.84	0.160	1.763	16.03
153		CO_2	751	769	7.29	14.78	0.160	1.868	16.97
154	2B	N_2	752	373	11.07	14.34	0.033	1.262	11.57
155			752	381	10.91	14.34	0.035	1.279	11.73
156		CO_2	752	382	11.68	14.34	0.035	1.193	10.94
157		N_2	752	381	10.99	14.29	0.035	1.265	11.60

* including vacuum correction

Table II

Thermal Conductivity of Air at 0°C

Investigator	Reference	Year	$k \times 10^5$ (cal./sec. °C cm.)
Kannuluik and Donald	(26)	1950	5.74
Keyes and Sandell	(32)	1950	5.82
Stops	(54)	1949	5.84
Taylor and Johnston	(56)	1946	5.66
Ubbink and de Haas	(59)	1943	5.84
Northdurft	(42)	1937	5.78
Hercus and Sutherland	(21)	1934	5.72
Kannuluik and Martin	(28)	1934	5.76
Eucken	(12)	1913	5.66 (extrap.)
		Average	5.76

Our data: 5.79, 5.78, 5.72, 5.73 (extrapolated to 0°C)

Average 5.75

Table III

Thermal Conductivity of Argon

Temp. (°C)	$k \times 10^5$ $\left(\frac{\text{cal.}}{\text{sec.}\,^\circ\text{C cm.}}\right)$	c_v $\left(\frac{\text{cal.}}{^\circ\text{C gm.}}\right)$	$\eta \times 10^6$ (poises)	$f = \frac{k}{\eta c_v}$
54	4.55	0.0745	244	2.50
360	7.54	"	396	2.55
558	8.98	"	478	2.52
576	9.26	"	485	2.56
688	10.44	"	527	2.66
689	10.52	"	527	2.68

Table IV

Accommodation Coefficients

Gas	Temp. °C	Accommodation Coefficient on Silver	Comparable Accommodation Coefficients on Platinum
Air	52	0.8	0.75 at 0°C (18)
Nitrogen	360-775	0.4 (av.)	- -
Carbon Dioxide	360-775	0.3 (av.)	0.5 at 25°C (64) 0.3 at 300°C (64) 0.6 at 300°C (57)
Argon	680	0.65	0.57 at 350°C (57)
Helium	680	0.13	0.17 at 400°C (57)

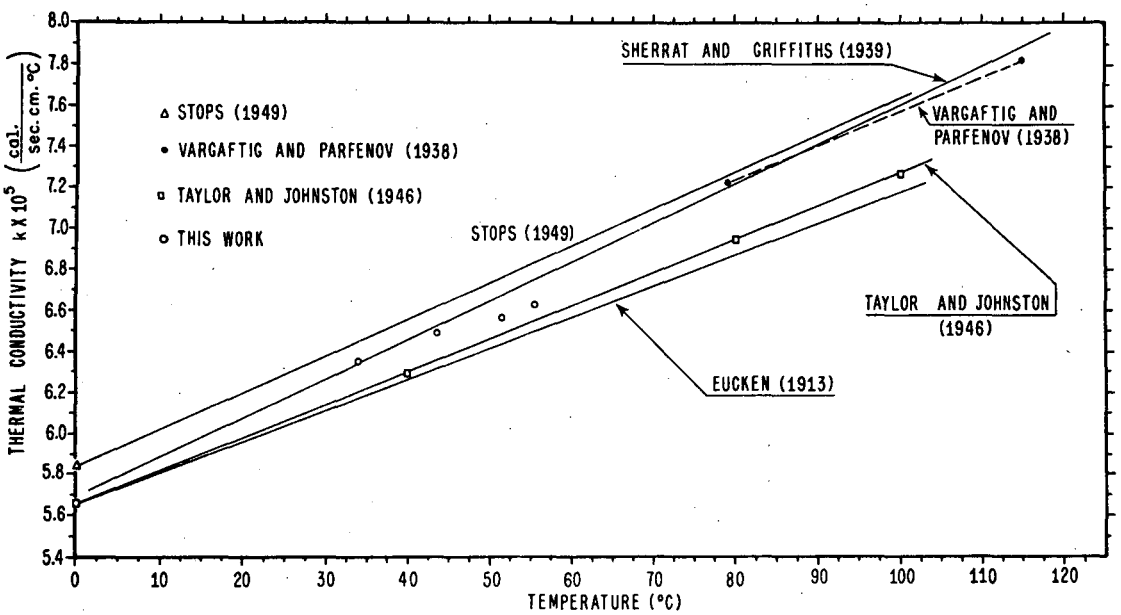

THERMAL CONDUCTIVITY OF AIR, VARIOUS INVESTIGATORS.

MU-6202

Figure 11

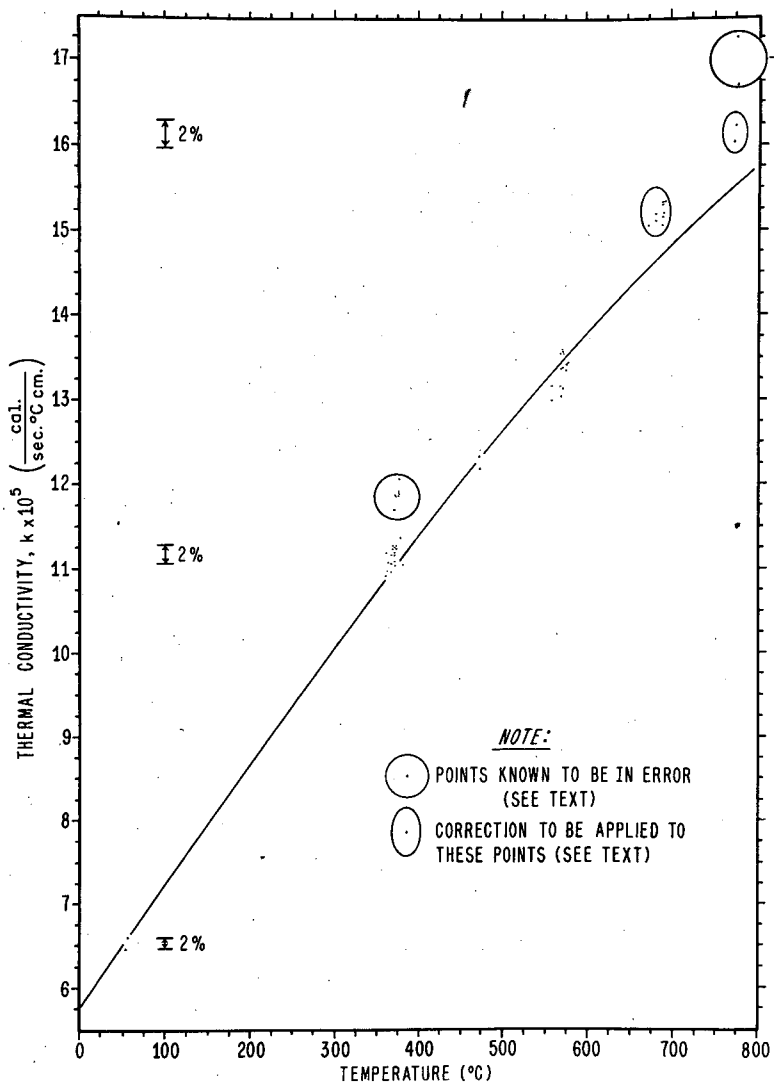

THERMAL CONDUCTIVITY vs. TEMPERATURE, NITROGEN

MU-6210

Figure 12

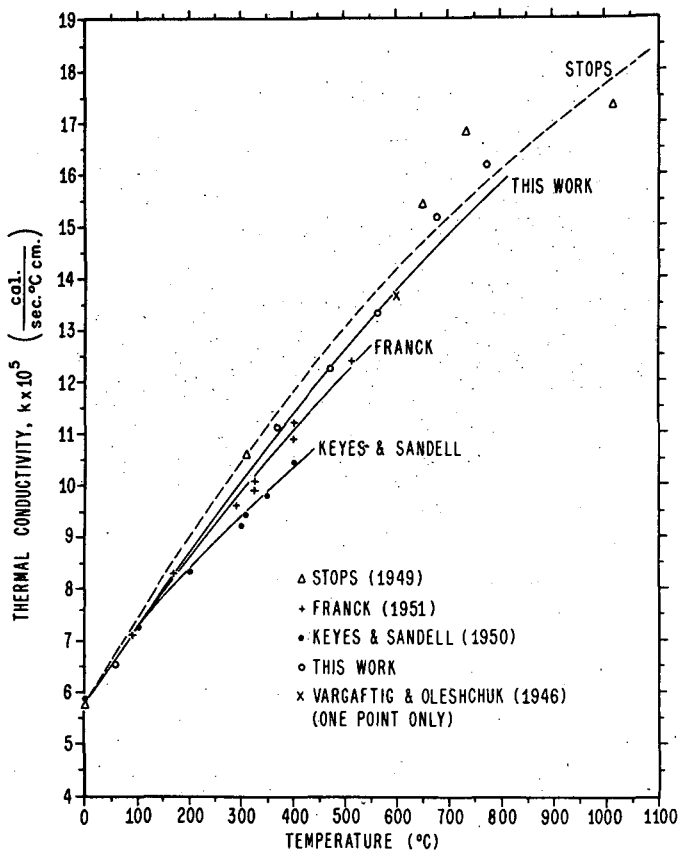

THERMAL CONDUCTIVITY vs. TEMPERATURE, NITROGEN, VARIOUS INVESTIGATORS.

MU-6212

Figure 13

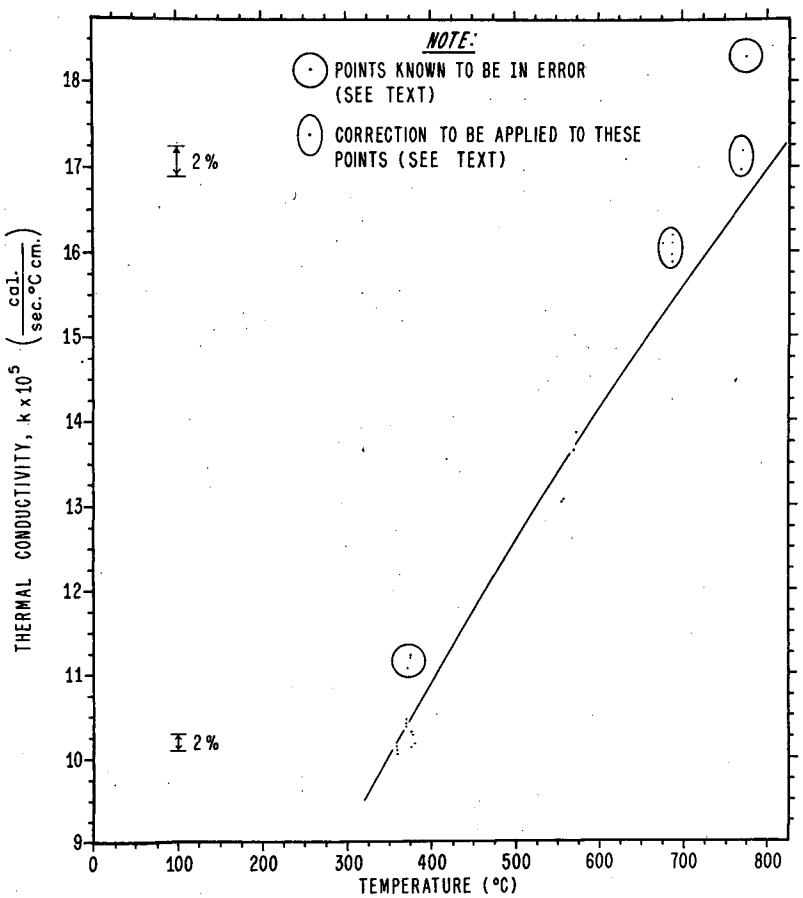

THERMAL CONDUCTIVITY vs. TEMPERATURE, CARBON DIOXIDE.

MU-6209

Figure 14

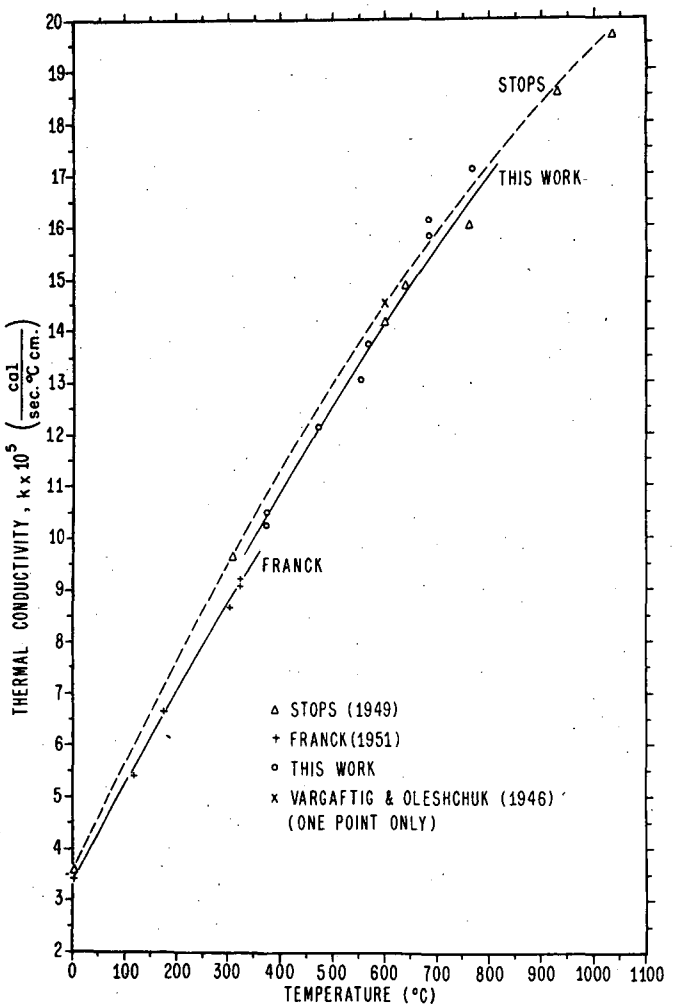

THERMAL CONDUCTIVITY vs. TEMPERATURE, CARBON DIOXIDE, VARIOUS INVESTIGATORS.

MU-6213

Figure 15

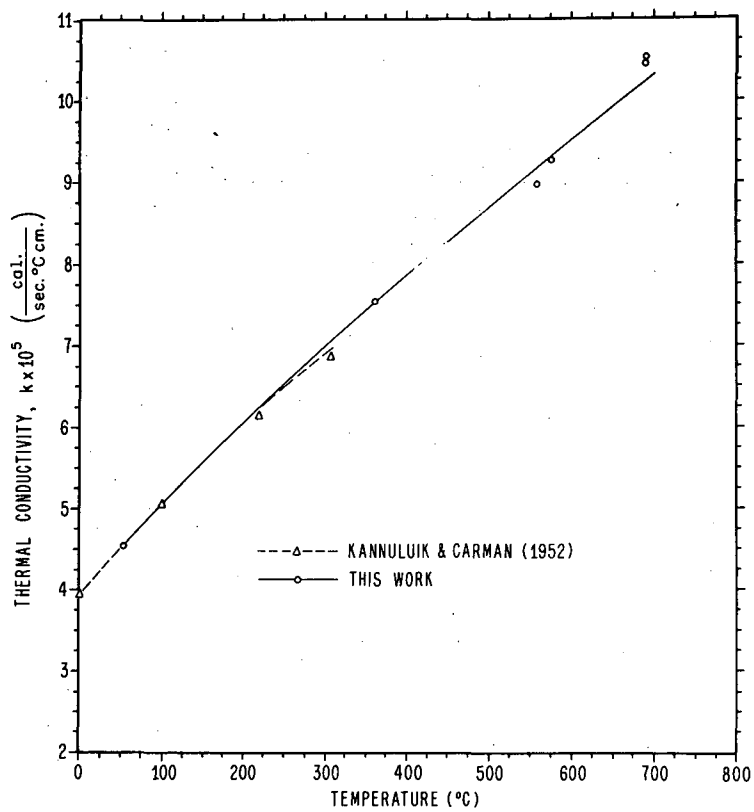

THERMAL CONDUCTIVITY vs. TEMPERATURE (ARGON)

MU-6208

Figure 16

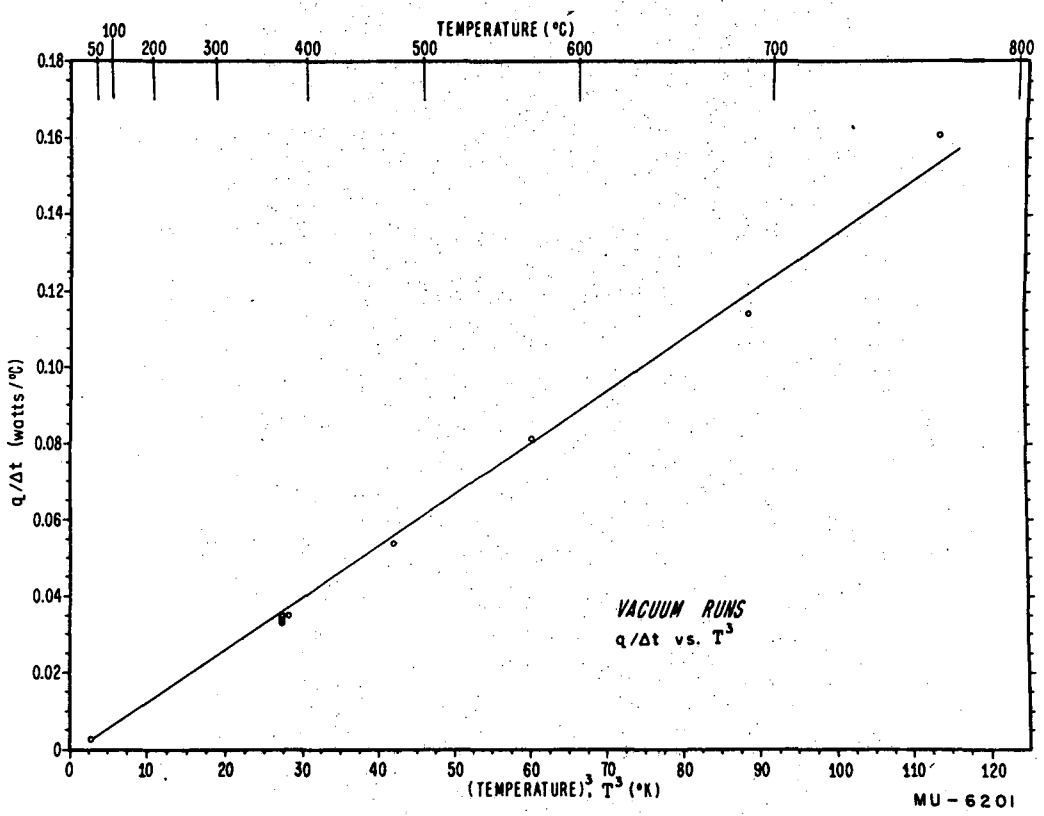
TEMPERATURE (°C)
100
50
200
300
400
500
600
700
800
0.18
0.16
0.14
0.12
0.10
0.08
0.06
0.04
0.02
0
q/Δt (watts/°C)
VACUUM RUNS
q/Δt vs. T³
0
10
20
30
40
50
60
70
80
90
100
110
120
(TEMPERATURE)³, T³ (°K)
MU-6201

Figure 17

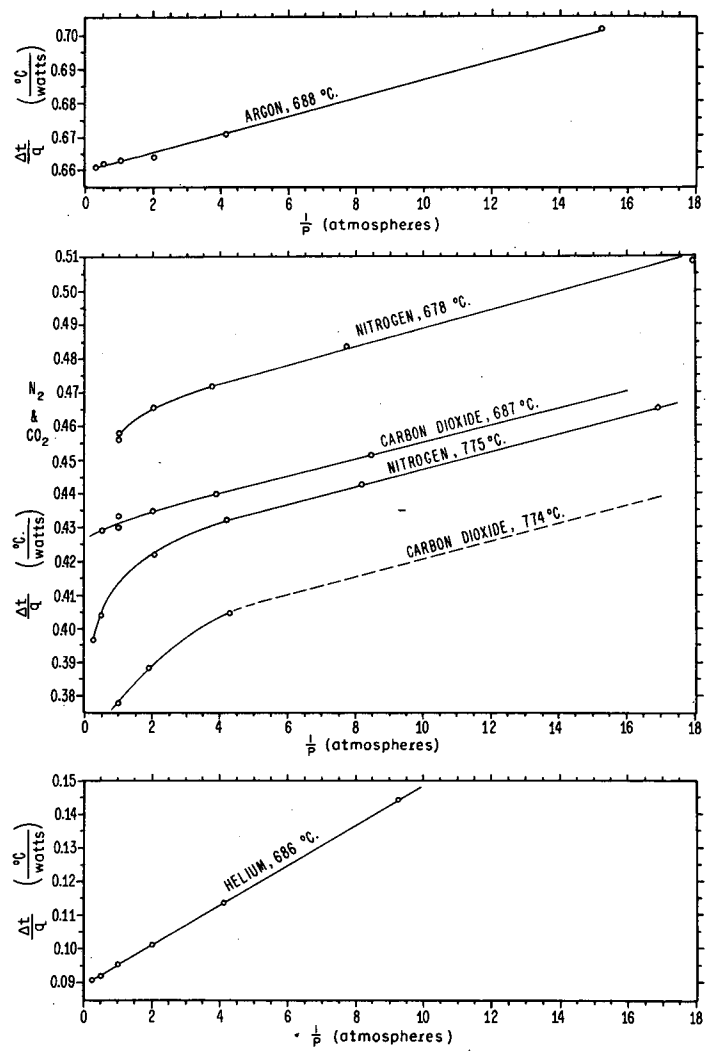

PRESSURE EFFECT $\frac{\Delta t}{q}$ *vs.* $\frac{1}{P}$

MU-6200

Figure 18

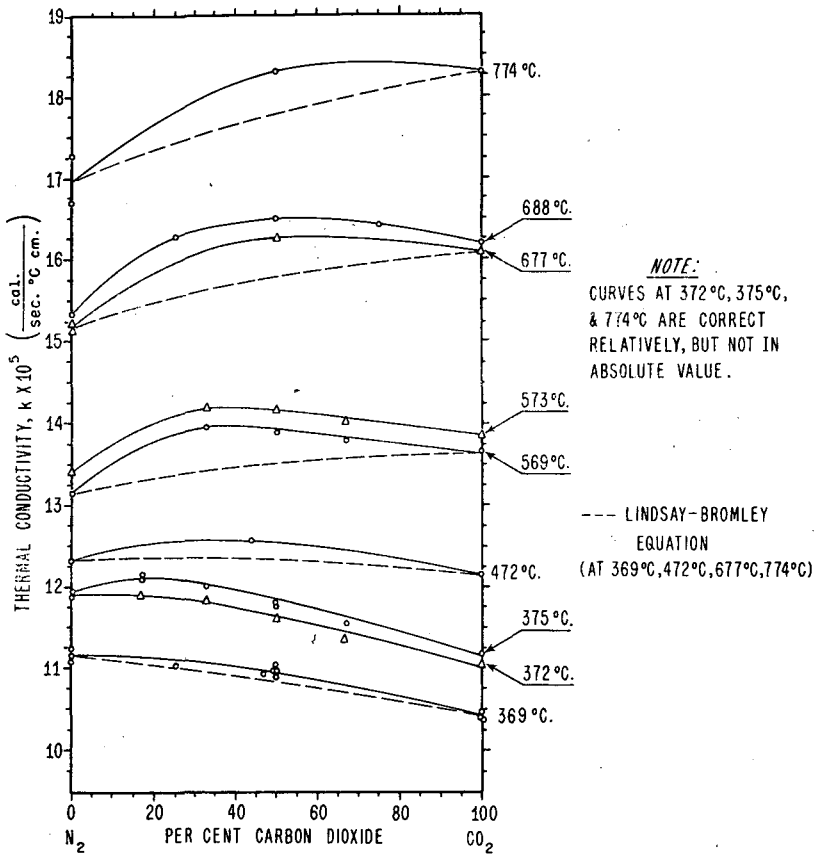

THERMAL CONDUCTIVITIES OF NITROGEN-CARBON DIOXIDE MIXTURES.

MU-6203

Figure 19

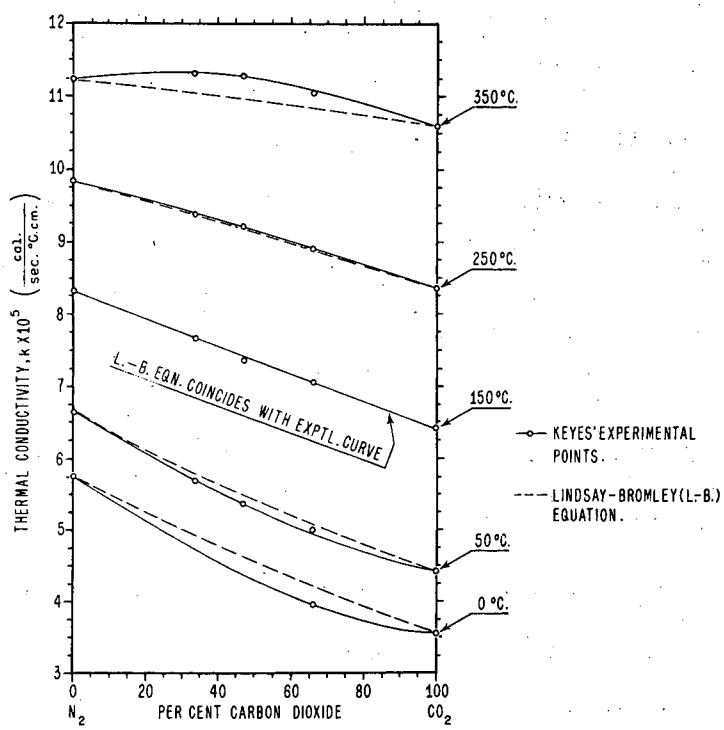

THERMAL CONDUCTIVITIES OF NITROGEN-CARBON DIOXIDE MIXTURES (KEYES)

MU-6206

Figure 20

IV. DISCUSSION

A. Corrections.

1. Vacuum Correction.

As mentioned previously, vacuum runs were necessary to correct for radiation and conduction across the supports. As Figure 17 indicates, $q/\Delta t$ versus the cube of the absolute temperature appears to be a straight line to a good approximation. This linear relationship leads one to believe that the emissivity is virtually constant over the whole temperature range considered. If the emissivity increased with temperature, the slope of the curve should also increase with temperature, since $q/\Delta t$ for radiation is proportional to an emissivity factor times the average absolute temperature cubed, for our moderately small Δt's ($<20°C$). The emissivity calculated from the slope of our plot is about 0.05.

The vacuum correction is only 0.003 watts/°C at 40°C, or about 0.3% of the net gas conduction. The $q/\Delta t$ vs. T^3 plot indicates even smaller corrections at lower temperatures. Consequently, true solid-solid conduction must be extremely small. However, it is mistaken to assume, as Keyes and Sandell[32] did, that the $q/\Delta t$ transferred in vacuum necessarily corrects completely for the heat transferred across the supports when gas is in the cell. Actually, even though the support is in good mechanical contact with the receiver and emitter, an appreciable, and probably a preponderant proportion of the heat is conducted in series across the support and gas spaces, one between receiver and support, and the other between support and emitter. The gas space between emitter and support is particularly narrow near the contact point between the two parts, and therefore offers low resistance to heat transfer. At still closer approach to the point of contact, conductive transfer through the gas takes place increasingly by a molecular rather than by a collision mechanism and so the conductivity

of the gas decreases. This partly offsets the effect of closer approach, especially at distances comparable with the mean free path at atmospheric pressure (about 10^{-5} cm at 25°C). When a high vacuum is applied to the cell, the conductivity of the small space between emitter and support becomes almost negligible, and heat is transferred through the gap chiefly by radiation (which is small at low temperatures). Consequently, the effective thermal resistance of the Lava support and its "gaps" becomes quite high and the measured heat transfer is not representative of what it actually is when the cell is filled with gas at atmospheric pressure.

To evaluate the degree of conduction across the supports, we assumed a flat emitter surface (a conservative assumption), and that the tip of each Lava support is a perfect hemisphere whose diameter is equal to the maximum diameter of the support. (The actual support is shown in Figure 1 and the assumed model in Figure 26). We then assumed only linear flow of heat. Actually the heat flow is somewhat greater since curvilinear flow occurs, but this does not affect the order of magnitude of the calculation. Integrating the conduction along hollow cylindrical elements, we obtained the total heat flow.

Conservatively, we neglected the reduction of the conductivity of air with decreasing gap dimension. It is recognized that the Lava tip and the surface are microscopically quite rough, so that they contact each other at more than one point. However, even this contact is poor from a thermal conduction point of view,[38] and anyway, solid contact is corrected for in the vacuum runs. Also, the existence of each rough projection of the tip or emitter surface implies a depression adjacent to it, so that one offsets the other with respect to the overall calculation. Finally, we (quite conservatively) ignored the contact resistance caused by a thin gas space at the flat end of the support

adjacent to the receiver.

For air at room temperature, our calculations indicate about + 0.3% error in the conductivity caused by neglecting the above effects in all seven supports. The extent of receiver surface area lost to (measured) gaseous conduction is about 0.086 square inches, or 0.2% of the total area, due to the fact that seven 1/8" diameter holes were drilled in the receiver in order to insert the Lava supports. In turn, this loss also reduces the apparent conductivity (based on a complete surface) by 0.2%. Consequently, the net effect of support conduction is negligible. This observation also holds at elevated temperatures.

The vacuum corrections vary from -0.3% at room temperature to -6% for Cell No. 1 and -8% for Cell No. 2 at 775°C. These corrections were found to be reproducible within 2 to 3% at 360°C, the only temperature at which they were rechecked, for all cell assemblies and even after exposure to 775°C. An error of this magnitude results in an uncertainty in the calculated gas conductivity of only 0.2% under the worst possible conditions (i.e., at 775°C in Cell No. 2 with the larger annulus).

2. Pressure Effects.

Two pressure effects were observed: convection and accommodation.

(a) Convection.

The cell was designed to eliminate convection in the annulus, but convection near one atmosphere was clearly detected as evidenced by the curves in Figure 18. There are two possibilities as to where the convection originated. One conceivable location is in the 1/2" gap between the top of the emitter and the bottom of the guard. Although the emitter and guard are at virtually the same temperature, the top of the receiver adjacent to the emitter is 5 to 10°C lower. Also, the vertical cell casing is another 5 to 10°C below the receiver temperature, and so there is a possible driving force of about 20°C.

The Grashof number ($= \frac{gD^3\beta\rho^2\Delta t}{\eta^2}$) for this condition is moderately small, however, amounting to 4000 at 50°C and 25 at 770°C for nitrogen, based on a D of 1/2". Normally convection should be extremely small for this range of Grashof numbers.[25] Furthermore the Grashof number changes to a great degree between these extremes of temperatures, and yet convection appears to be virtually absent at 50°C as determined by pressure runs but quite appreciable at 670° and 770°. Also at 770°C the smaller Grashof number should induce less convection than at lower temperatures, which was opposite to what was observed. Finally, convection did not show a consistent trend with variation of Δt, as would be expected if the convection originated at the gap between the emitter and guard.

The second possibility is that convection originates in the pipe used for evacuating and filling the cell. This pipe extends vertically upwards from the hot furnace to the colder atmosphere of the room. Its large diameter (necessary to permit a good vacuum pumping speed) allows large convection currents to flow which are not halted at the horizontal section of the pipe just above where it enters the cell, nor are they blocked by the heat guard, even though there is only a small annular passage (1/8") between the guard and the cell casing. These convection currents are apparently strong enough to penetrate to the top of the emitter and receiver and increase the heat transferred across them. The Grashof number calculated on the basis of the pipe diameter and the temperature difference between the furnace (at 370°C) and room (at 25°C) is 100,000, which is in a region of high convection.[25]

The actual convection effects above 300°C as evidenced by pressure plots showed random variations independent of temperature from zero (in the case of the argon pressure run and several nitrogen

and carbon dioxide runs) to 1.3 percent in others, probably because of experimental uncertainty. No effect was found at room temperature. The above observations also fit our hypothesis, since the temperature gradient available for convection at 770°C is only about twice that available at 380°, and the physical properties at the higher temperature are such as to make convection weaker than at the lower temperature. Consequently the difference in the degree of convection at the two temperatures should not be marked. However, the temperature gradient at 50°C is only 25°C, or about one-thirtieth of that at 770°C.

To apply a reasonable correction to each run, the average measured degree of convection (0.5%) was deducted from the $q/\Delta t$ for nitrogen, carbon dioxide, and argon at one atmosphere and at all temperatures higher than 60°C (i.e., at 350°C and above) after correcting for radiation. In this manner, the maximum error introduced in the conductivity is + 0.8% in some runs, and the probable error is less.

Note that the correction as applied actually represents the difference between the result ($q/\Delta t$) at one atmosphere and that obtained by extrapolation of the $\Delta t/q$ vs. $1/P$ plot to $1/P$ equals zero (see below). Thus, we actually correct for the difference between convection (tending to increase the apparent conductivity) and accommodation effect (tending to reduce the apparent conductivity). The degree of convection alone averaged one percent, and varied more or less at random from zero to two percent, although the highest value occurred at the highest temperature.

(b) Accommodation - Temperature Jump Effect.

The accommodation-temperature jump effect which is usually considered in the case of hot wire cells is generally ignored in the case of concentric cylinders. Keyes and Sandell[32,46] for example, do not even mention it as applying to their cell. However,

as shown in the Appendix, this effect is of the same order of magnitude in our (and Keyes and Sandell's) apparatus as it is in the usual hot wire cells, primarily because of our small annular space, and the fact that the ratio of the radii of our cylinders is close to one. In cases such as Kannuluik and Carman's "thick-wire" cell,[27] wherein the inner (wire) radius is relatively large (0.075 cm) and yet the ratio of outer to inner radius (4.66) is not close to unity, the effect is considerably smaller (their effect is only 1/3 of ours). Furthermore, as shown in the Appendix, the accommodation effect is most evident at high temperatures, and particularly at low pressures, because of the longer mean free path, and consequently the magnified molecular effects.

At 52°C, the accommodation effect correction is extremeley small for air (and presumably nitrogen), amounting to less than 0.1%. The corresponding accommodation coefficient is approximately 0.8, as calculated from our data. The corrections increase with temperature, and the averages range from about 0.3% at 360°C for nitrogen and carbon dioxide to about 0.7% for nitrogen and 1.3% for carbon dioxide at 775°C. Thus, the effects are not negligible. In the case of helium, the physical properties, notably the low (0.13) accommodation coefficient, are such as to introduce large error (-6.3%) if accommodation is not considered.

For interest, approximate accommodation coefficients obtained from Figure 18 by means of Equation (7) in this paper are listed (Table IV). These appear to be reasonable, as evidence by comparable values included in the table for accommodation on platinum.[18,57,64]

3. Effect of Temperature Gradient (Δt).

The effect of Δt on apparent conductivity in the range of Δt = 2-3°C to Δt = 15-25°C was found to be smaller than that attributable to random experimental scatter, i.e., no more than one percent.

Since most of our data by far were measured at a Δt of 7° or less, error due to possible variation of conductivity with Δt is well below one percent (probably only 0.2% or less). The reasons that one might expect to find an effect of Δt in our cell are possible convection at the gap above the emitter, which was shown to be unlikely, or excessive temperature elevation of the emitter heater lead wires above that of the emitter and guard. Some temperature difference, of course, must exist between the heater wire and the emitter surrounding it, in order that heat may flow. If this difference is high, appreciable heat (unaccounted for in the calculations) will flow up the cell and cause the calculated conductivity to be too high.

Keyes and Sandell[32,46] found a marked effect of Δt on $q/\Delta t$ even at $\Delta t \leq 2°C$ in their apparatus. Convection was clearly absent at atmospheric pressure as evidenced by their ability to obtain conductivity measurements up to 150 atmospheres. They attributed this Δt effect primarily to heater lead wire temperature elevation, and to some convection at high pressures, and were forced to make accurate measurements down to $\Delta t \leq 2°C$ and extrapolate to $\Delta t = 0$. This correction, for instance, for a steam measurement at 350°C and 73 atmospheres [$k = 13 \times 10^{-5}$ cal./(sec.)(°C)(cm)] amounted to 4% of the $q/\Delta t$ measured at $\Delta t = 2°C$ and so demanded a high precision in the measured $q/\Delta t$'s. They empirically found a linear relationship between $q/\Delta t$ and $q^2/\Delta t$ at $\Delta t > 2$, so that their final results depend upon whether this linearity also held at Δt's close to zero. To eliminate these extrapolations, our emitter heater was designed using a much larger wire surface than Keyes and Sandell's, to lower the required heater wire temperature for a given emitter temperature. Although we used a nichrome wire heater, the leads running up the length of the emitter were platinum to minimize the joule (I^2R) heating effect over its

length. We also brought the tube enclosing the lead wire into close contact with the silver emitter cylinder by means of a small silver plug closely enveloping the tube and screwed to the emitter (Figure 1).

B. Conductivities of Gases.

1. Air.

The conductivity of dry air was measured first to see if reasonable data could be obtained from the cell. The results are best seen in Figure 11, in which conductivity is plotted versus temperature. Several curves are drawn for comparison, based on the data of Stops,[54] Taylor and Johnston,[56] and Eucken.[12] Our data fall between the extremes of these investigators. Extrapolation of our results to 0°C by means of Taylor and Johnston's slope give values (average = 5.75 x 10^{-6}) which are close to the average (5.76 x 10^{-5}) of recent typical investigators (See Table II).

2. Nitrogen.

The values for nitrogen areplotted in Figures 12 and 13. The values fall in the range between most investigators' results up to temperatures at which others have made measurements. Note that Keyes and Sandell's data are admittedly too low at 100-400°C, as Keyes admits in the post-paper discussion of a later article.[33] It is conceivable that a part of this effect could be attributable to their failure to take the accommodation-temperature jump effect into account, as mentioned above. However, they did not present sufficient low pressure data (0-1 atm.) to permit us to draw any conclusions regarding the magnitude of their accommodation effect.

Above 600°C, the only other data available are those of Stops, which are admittedly only a first attempt to obtain high temperature data.[53] Note, for example, the scatter of several values on Stops' nitrogen curve. Our results are clearly lower than Stops' up to 600°C. Above 600°C our uncorrected points reach his smoothed curve and exceed it slightly (about 1.5%). However, Stops' data scatter badly in this range and the placement of his curve is arbitrary. In fact, in his

thesis[54] the smoothed values he lists at 700°C and 800°C are respectively 2% and 3% above the corresponding points on the smoothed curve presented in his paper.[52] It is interesting, but probably only coincidental, that at the two temperatures at which our points appear high, viz. about 670 and 770°C, Stops' measured values were also high, viz. 5% and 8.4% above his smoothed curve. He was able to make a measurement near 1000°C, which brought his smoothed curve down. The point at 1000°C was actually subject to greater error, as Stops indicates in his thesis[54] because of his difficulty of maintaining steady state conditions at high temperatures as well as the large radiation correction (20%). He offered no explanation as to the distribution of his three highest points (i.e., whether any improvement in the method was made after obtaining the two deviating points). It is also noted that Stops did not correct for radiation by making measurements in vacuo. Instead, he used Helfgott's[19] relation for the emissivity of platinum as a function of temperature.

It should be noted that two series of our experimental points at 360°C and at 770°C cluster above different values approximately 6% apart. The upper ones are clearly in error and the conditions under which these were obtained give a possible clue as to why our conductivities at elevated temperatures are apparently high. Measurements were first made near 50°C, and then the cell was taken apart for examination. After re-assembly the same results were obtained at 50°C (within one percent). This second set of readings covered the range from 50°C to 560°C, and then the cell was disassembled to repair a burned-out heater lead. After re-assembly, runs at 360° and 560°C were repeated, and the results checked the previous values quite well. Measurements were next made at 680° and 770°C and then the temperature was cut to 360°C to obtain a final check. This time the 360°C result was

about 5% higher than before. When the cell was dismantled, it was found that the previously smooth, polished silver surfaces were now rough and full of unbroken "bubbles" or blisters. This change in the surface did not change the emissivity appreciably; vacuum runs at 360°C before and after exposure to high temperatures agreed to better than 3%, corresponding to an error of less than 0.1% in conductivity calculated using these radiation corrections. The roughness, however, estimated at several thousandths of an inch, apparently increased the cell constant by decreasing the annular spacing between the emitter and receiver. Thus higher apparent conductivities were obtained based on the original cell dimensions. This roughness is attributed to the tendency of trapped gas in the cast silver to outgas at elevated temperatures. The solubility of oxygen in molten silver is high, and decreases sharply, upon solidification of the metal.[39,49] During casting, part of this oxygen evolved when the silver freezes is mechanically trapped in the silver, resulting in a somewhat porous structure. When the temperature is raised to about 600° to 700°C, the combination of increasing pressure of the trapped oxygen and decreasing strength of the silver causes small bubbles to form at the surface, particularly when the cell is under a vacuum. The possibility of outgassing was considered before the equipment was constructed, but because of inability to obtain a large block of silver cast in vacuum within a reasonable period of time, certrifugally cast silver was used in its place. It was thought that the dissolved oxygen would have been forced out during centrigugation at the solidification point.

The cell was re-machined after the first series of high temperature runs to produce smooth surfaces again, measured, and assembled once more. This time the cell was not exposed to high vacuum, and even the time at

moderate vacuum (2 mm Hg) was minimized. The cell was brought to steady state rapidly by additional heaters in the tin bath, and measurements were made as quickly as possible at 360°, 680°, and 770°C. The results at 360° and 680°C checked the previous ones quite closely (better than one percent), but those at 770°C fell six percent below the previously measured ones. Unfortunately just before re-checking at 360°C, the heater leads shorted out. After disassembly, the receiver and emitter surfaces were examined and only slight roughness was observed. The area of roughness was much smaller and the depth of the "bubbles" appeared smaller. The silver felt smoother over most of its surface than it did after the previous exposure to 770°C. Also the cell annulus was 30% wider than before, which condition should reduce the percentage effect of roughness on the cell constant.

To serve as a final check, the emitter heater leads were fused together, the shell was hard-soldered instead of welded to speed the process of installation, and data were then taken at 370°C (See Runs 154, 155 and 157). This time the results were 3% higher than the average of the previous "good" data (i.e., conductivity measurements before the cell was exposed to high temperatures). At most we might expect about one percent random variation in these last readings as compared with the earlier ones. Consequently, the exposure to high temperature affected even this last group of results. As a further check, the cell was dismantled and micrometer measurements made on the emitter and receiver. No appreciable distortion had taken place. Then the average annular width was measured by the technique described in the Appendix. The width had decreased from 0.03341" to 0.03277", or by 1.9%, which should decrease the cell constant and therefore increase the conductivity based on it by about 1.9%. The difference

between 3% and 1.9% is attributed to random error in the conductivity measurements. Since the annulus measurement is more precise, it is reasonable to assume that the actual increase in conductivity was about 2%. On the basis of the above, it is estimated that the results at 680°C are about 2% high, and those at 780°C are about 2.5% high in comparison with the lower temperature data.

3. Carbon Dioxide.

The data for carbon dioxide show about the same relationship to Stops' data as do those for nitrogen. The discrepancies in the measured conductivities before and after each re-assembly of the cell were greater than those for nitrogen or argon (see below). For example, runs made before Run 53 in Cell No. 1B (before disassembling this cell) yield an average conductivity of 10.24 corrected to 374°C. Those made after Run 52 in Cell No. 1C (after re-assembly) average 10.49. Thus the two values differ by 2.4%. Nitrogen conductivities under the same circumstances differ by 0.7%. At 570°C, conductivities measured in Cell No. 1B and No. 1 C differ by 3.6% in the same sense, while comparable nitrogen conductivities differed by 1.1% and those of argon by 0.7% in the same direction. In addition, the discrepancy between the average of all measured conductivities at 375°C and those measured directly after exposure to high temperatures is 7.5%. However, the comparison between the values at the same temperature measured just before and just after exposure to the high temperature (in Cell No. 1C) was 6%, or the same as for nitrogen. This would indicate that the values obtained in Cell No. 1C are probably more reliable than those in Cell No. 1B. Another indication of this conclusion is that after the second exposure to high temperatures in Cell No. 2, the conductivity of carbon dioxide at 374°C was 5.5% above those measured in Cell No. 1B, but only 3% above the corresponding ones in Cell No. 1C. This latter

value agrees well with the nitrogen discrepancy of 3% cited above. By the same token the higher values at 570°C measured in Cell No. 1C are probably more reliable than the corresponding ones in Cell No. 1B. The discrepancies observed are attributed to large random errors, since measurements made using carbon dioxide were considerably fewer than those with nitrogen, particularly at 570°C.

It should be noted that gaseous carbon dioxide can radiate (emit and absorb) thermal energy.[38] The degree of radiation increases with increasing thickness of the gas layer and with increasing partial pressure of the gas. Since our annular width is small and since we extrapolated our carbon dioxide results from a pressure of only 1/4 atmosphere (see above), the effective gaseous emissivity is small. In addition, radiation and re-radiation takes place on silver walls of low emissivity. Consequently the carbon dioxide radiation is believed to be negligible in our determinations.

4. Argon.

No other investigators have taken data up to 700°C. The theory of Chapman[9] predicts that the ratio $k/\eta c_v \equiv f$ for elastic, spherical molecules is about 2.5 and is independent of temperature. Kannuluik and Carman[27] found that indeed this ratio for the inert gases helium, neon, argon, krypton, and xenon appeared to be independent of temperature in the range of -183°C to 306°C although he observed that the f ratios apparently increased with increasing molecular weight among the inert gases, from 2.43 (helium) to 2.58 (xenon). Our data for argon are shown in Table III, and are plotted in Figure 16. At room temperature our data agree with those of Kannuluik and Carman, but appear to diverge at the highest temperature at which the other authors made measurements (306°C). (The smooth curve drawn through their data is

their own.) If we assume that the f ratio truly remains constant with temperature as Kannuluik observed at lower temperatures, then our f values are 5% high at 688°C, although reasonably consistent below that temperature. It is fairly likely that our data for all gases are 2 to 3% high at 680°C, but this discrepancy in the case of argon appears rather large. It may be due to experimental error in the measurement of this particular gas since relatively few repeat determinations were made, but it may also be attributable to an error in the viscosity used. The viscosities listed in Table III were calculated from Bromley and Wilke's tables[6] based on Hirschfelder, Bird, and Spotz' papers.[22-24] The latter authors' force constants were determined from experimental viscosity data at relatively low temperatures (below 400°K) and the viscosities predicted by them differ by several percent from experimental data at higher temperatures. (See Reference 24, Table 8a)

5. Helium.

The helium data were taken primarily as a means of checking the pressure effect to substantiate the idea that temperature jump-accommodation was actually causing the effect observed. It was known that helium has a lower accommodation coefficient than nitrogen and most other gases on platinum and several other metals[44,57] and so it was thought that helium would also show lower accommodation on silver. Such was the case.

Because of the primary object mentioned above, the conductivity was measured only at 686°C, using helium from a cylinder conveniently available. The cylinder did not clearly indicate its source, and so the purity could not be readily checked (see Appendix). Consequently the conductivity of helium is listed, but cannot be relied upon too heavily. The $f \equiv k/\eta c_v$ ratio calculated on the basis of our measured conductivities equals 2.49 or 2.38, depending upon whether the Hirsch-

felder prediction[24] for viscosity is used (0.0418 cps.) or the viscosity data of Trautz and Zink[58] (0.0439 cps.). Kannuluik and Carman[27] obtained an average ratio of 2.43 at -183°C to 306°C.

Convection was totally absent in the helium runs, even at 4 atmospheres.

6. Nitrogen-Carbon Dioxide Mixtures.

The mixture results are plotted in Figure 19. The data clearly indicate that in this range of temperatures (above 360°C) the conductivity curve reaches a maximum value, several percent higher than either pure component. In comparison, note that the mixture data of Keyes[33,34] (Figure 20) bow downward below 150°C, even though no minima occur. Apparently at low temperatures the mixture data show a negative departure from linearity between the pure components; at some intermediate temperature (slightly above 150°C) the relationship reaches linearity; and then at higher temperatures positive deviations from a straight line are obtained. This last effect is shown both in our data and Keyes' data in Figures 19 and 20. It is also interesting to observe that at about 500°C, the conductivity of carbon dioxide reaches that of nitrogen and exceeds it to an increasing degree at still higher temperatures.

The Lindsay-Bromley correlation presented earlier was applied to our data, and is shown at the particular temperatures of 369°, 569°, 688° and 774°C, in Figure 19. Since viscosity ratios (nitrogen to carbon dioxide) are required, all viscosities were taken from the Bromley-Wilke paper[6] for consistency. The maximum deviations of the Lindsay-Bromley equation values from ours are -1% at 369°, -1.1% at 372°C, -1.9% at 375°C, -1.5% at 472°C, and about -3% at the higher temperatures. By comparison, the equation shows a -1.8% deviation from Keyes' experimental values at 350°C. In his report, Keyes[34]

showed the Lindsay-Bromley plot as curving in the direction opposite to that which we calculated it to be. In our calculations, we used the viscosities from the Bromley-Wilke paper, the viscosities from this same Keyes report, and we also made a third calculation using Keyes' tabulated specific heat data in the Eucken relation as outlined in Lindsay and Bromley's article. All of these calculations resulted in almost identical curves. We conclude that Keyes' calculations are probably in error.

While the discrepancies due to the Lindsay-Bromley correlation are not serious, nevertheless they indicate a trend which may be even more pronounced in other mixtures at high temperatures. It would certainly be desirable to measure the conductivity of other gas mixtures at elevated temperatures to confirm these observations.

It should be noted that the absolute values of our mixture data at 372°, 375° and 774°C are known to be high by about 6%, for the reasons outlined in an earlier section. However, all the data at each of these particular temperatures are high by the same factor, and so the mixture curve should show relatively the correct shape. In fact, the form of the curves at 372°C and 375°C is probably more reliable than that at 369°C, owing to their smaller experimental scatter. The curve at 774°C is less reliable because the cell constant was probably changing with time (see below). Note that two values are plotted for pure nitrogen which are 3.3% apart. The data at 569° and 573°C are probably the most reliable of all since they show excellent independent agreement in form.

C. Evaluation and Conclusion.

1. Random Errors.

The various random errors which our measurements are subject to are listed below. Errors of less than 0.1% are considered negligible here.

(a) Cell Constant.

There is negligible error in the measurements of all lengths and the emitter cylinder diameter. The annulus measurement is subject to ±0.4% maximum error in the first cell, but to only ±0.2% in the second cell because of refinements in technique. The error introduced by simplifying the conduction equation (see Part I) is ± 0.3%. Strictly speaking this is not a truly random error, but its direction is not known, and so it is treated as random for simplicity.

The overall cell constant and the conductivities calculated therefrom are thus in doubt by about ±0.6%.

(b) Temperature.

Temperatures based on the Bureau of Standards calibrated thermocouples are known to ± 0.5°C. However, since a 1°C increase in temperature results in a 0.1 to 0.15% increase in conductivity, the temperatures were listed to the nearest degree, introducing negligible error in the conductivity.

(c) Thermocouple Calibrations.

The dE/dt calibrations for the thermocouples are known to about ± 0.3 - 0.5%, which affects the conductivity to the same degree.

Intercalibrations between couples were usually reproducible to ± 0.2 microvolt, but occasionally varied by ± 0.5 microvolt. Under the latter circumstances, the error in a Δt of 6°C as well as in the calculated k was ± 0.8%. However, conductivity measurements were repeated several times under the same conditions before and after interchanging thermocouples. Consequently conductivity values show

an appreciable spread of a few percent at each condition, yet the error in their averages is much smaller because of the compensatory nature of intercalibration errors. A reasonable estimate of the residual error caused by intercalibrations is ± 0.3% at a Δt of 6°C and less at higher Δt's.

(d) Heat Input.

Errors in current and voltage measurements are negligible. The corrections due to voltage drop in the lead wires are from 0.4% to 1.0% at 40°C to 770°C respectively. These are know accurately within ±0.1% based on the total heater voltage drop.

(e) Vacuum Corrections.

The maximum vacuum correction (8%) for radiation and support conduction occurs at 774°C, introducing at most 0.2% uncertainty into the final conductivities, as detailed in a previous section.

(f) Pressure Corrections.

As discussed above. 0.8% is the maximum error in correcting for convection. Correction for accommodation is included in this, as mentioned previously.

Adding all these errors, the maximum additive error is 2.3%. Allowing for randomness in the individual errors, the probable error would be about one percent.

2. Reliability of Cell and Data.

Here we consider the errors in a particular direction as distinguished from the random errors discussed above.

A possible error is caused by neglecting the effect of Δt on the conductivities calculated therefrom. However, the conductivities so calculated may be high by no more than 0.2%, as pointed out above.

It was shown that conduction at the supports probably produced

negligible effect. If there is a small effect, it would also tend to make the calculated conductivities too high.

Departure of the inner cylinder from concentricity also yields high conductivities. The largest expected eccentric displacement of the inner cylinder (including the full displacement possible owing to differential expansion between the silver and Lava supports) is 0.002" (at 770°C). Using the customary calculation for eccentric cylinders (e.g. see references (46), (60)) we have:

$$k(\text{correct}) = \frac{q \ln \left\{ \dfrac{\sqrt{(r_2 + r_1)^2 - e^2} + \sqrt{(r_2 - r_1)^2 - e^2}}{\sqrt{(r_2 + r_1)^2 - e^2} - \sqrt{(r_2 - r_1)^2 - e^2}} \right\}}{2\pi L \Delta t} \tag{11}$$

and

$$\frac{k(\text{correct})}{k(\text{apparent})} = \frac{\ln \left\{ \dfrac{\sqrt{(r_2 + r_1)^2 - e^2} + \sqrt{(r_2 - r_1)^2 - e^2}}{\sqrt{(r_2 + r_1)^2 - e^2} - \sqrt{(r_2 - r_1)^2 - e^2}} \right\}}{\ln (r_2/r_1)} \tag{12}$$

where e= eccentricity, and r_2, r_1, are the radii of the larger and smaller cylinders respectively. The maximum error introduced into our calculated conductivity is 0.3% at 770°C, and considerably less at lower temperatures.

The most important directional errors occur at 680° and 770°C. The nitrogen and carbon dioxide results were clearly too high during the first determination at 770°C, (Cell 1) and were rejected. However, the results at 680°C both in Cells 1 and 2 also seem to be

several percent high, as noted in earlier discussion. We also observed that at 770°C the measured conductivity apparently changed between the first measurement and one made 8 hours later, after repeated applications of moderate vacua (0.5 to 200 mm). This result may have been merely a large random error, but likely indicates increasing blistering of the cell. During the second series of runs at 770° (Cell 2) the two determinations checked each other well.

Based on the above observations, it appears that some blistering probably occurred on the silver at 680°C, and this process was accelerated at 770°C, particularly under vacuum. During the Cell 2 measurements at 770°C, the observations were made allowing less time to elapse and utilizing vacuum only to purge the cell between nitrogen and carbon dioxide runs.

On the basis of the above, it is estimated that our data are 3% high at 770°C and 2.5% high at 680°C. Our smoothed curves for carbon dioxide, nitrogen, and argon which were drawn giving more weight to the points at temperatures below 680°C also show about these deviation from the high temperature experimental points. The data at other points are subject to the random error of about 1% where numerous repeat determinations were made, and up to about 1.5% where relatively few data were taken.

3. Suggested Conductivity Values for Nitrogen and Carbon Dioxide.

Based on our smoothed curves and those of other workers shown in Figures 13 and 15, we have compiled a list of thermal conductivities for nitrogen and carbon dioxide from 0° to 1000°C (Table V) which we consider the best data currently available. No attempt has been made to fit the curve critically to all values in the literature. Most of the values are taken from our curves. The justification is

Table V

Suggested Conductivities -- Nitrogen and Carbon Dioxide

Temp. (°C)	Thermal Conductivity, $k \times 10^5$ (cal./sec.°C cm.) Nitrogen	Carbon Dioxide
0	5.76	3.50
100	7.25	5.4
200	8.7	7.2
300	10.1	9.1
400	11.4	10.9
500	12.6	12.6
600	13.8	14.1
700	14.9	15.6
800	15.8	17.0
900	(16.6)	(18.1)
1000	(17.3)	(19.1)

that the shapes of these curves are the most reasonable to use, since they parallel Stops' curves closely at all temperatures, and Stops is the only other investigator who has measured conductivities from 50° to 800°C. Moreover most of our systematic errors are such as to yield too high a conductivity. Therefore it is believed that Stops' data, which are above ours, are probably too high. Furthermore, our values appear to fall in the midst of most investigators' results at lower temperatures, unlike Stops' which are higher than the others.

At temperatures above 770°C, our curve was extrapolated to a continuing smooth curve parallel to Stops'. Estimates made from these curves are, of course, uncertain, and so they are bracketed in the table. Below 50°C for nitrogen, and below 360°C for carbon dioxide, we extrapolated our curves smoothly to the average values of others at 0°C.

4. Suggestions for Improvement.

(a) Corrosion.

As had been anticipated, the stainless steel was appreciably corroded by the tin. The sharp edges of the propeller were completely corroded away after several days of operation at 350°C. However the smooth agitator shaft was not affected even after several weeks at this temperature and a week at 570°C. Likewise the stationary parts, such as the stainless cell casing and the tin bath container showed virtually no corrosion under these conditions. After about a week at 670°C and three or four days at 770°C followed by two weeks at 350°C, all stainless parts were badly corroded, presumably due to the high temperature. The agitator shaft had lost 1/8" of its diameter, the 3/16" wall of the stainless steel can had corroded down to about 1/16" in spots, and the stainless cell jacket had lost about 1/8" of its diameter.

The first stainless steel propeller was replaced with a propeller

fabricated of titanium scraps in the Radiation Laboratory shops. This material was suggested by the Liquid Metals Handbook[37] based on a more detailed review[30] but showed extensive corrosion after exposure to 350°C and 570°C for a few weeks. The final material used for a propeller was molybdenum, based on Brewer's recommendations.[3] After exposure to 670°C, 770°C, and 360°C as outlined above, corrosion appeared inappreciable.

Since fabrication of a molybdenum can and cell casing would be difficult and expensive, it might be worthwhile to replace the tin bath with a massive block of copper or graphite to serve as a temperature equalizer and stabilizer. The block could be bored out to fit the cell closely and protected from oxidation during use by a steady flow of some inert gas (nitrogen, argon, etc.)

(b) Thermocouples.

The apparent change in calibration correction between emitter and receiver platinum thermocouples introduced a variable error. In most cases, interchanging thermocouples and then returning them to their original positions as described above resulted in a discrepancy of from zero to 0.2 or 0.3 of a microvolt. This caused an error of 1% or less if the Δt across the cell was 3°C or more. However, occasionally the discrepancy was 0.5 to 0.6 of a microvolt. In these cases the Δt across the cell had to be 6°C or more to limit the error to 1%. This change in apparent calibration is attributed to slight mechanical strains caused by pulling the thermocouples out of the wells and re-inserting them. The free ends of the wires were barely long enough to do this conveniently. Consequently it would be desirable to employ longer platinum wire couples from the hot junction to the ice bath to minimize strains in the wires while inter-calibrating the couples.

(c) Convection.

To obviate the need for "pressure-effect" runs at low temperatures and to make extrapolation to infinite pressures simpler at high temperatures, where the accommodation effect is appreciable, convection should be eliminated. In principle, leading the conductivity cell outlet pipe downward from the interior of the furnace to the exterior should accomplish this aim, but would require major furnace revisions. It might be feasible to provide baffles within the pipe itself, and a series of baffles within the cell casing to deflect any strong convection currents from moving downward into the emitter receiver annulus area. Still another possibility would be to enlarge the furnace opening where the pipe emerges and surround the pipe with auxiliary electric heater windings and insulation to keep the pipe at or near the furnace interior temperature.

(d) De-Gassed Silver.

The apparent trend in the data towards erroneously high conductivity results above 600°C has been attributed to the blistering of the silver cell after exposure to high temperatures caused by outgassing. The most important step in reconstructing the cell would be to provide silver stock which has been kept under high vacuum for a considerable period while molten and then cast in a vacuum. A cell machined from such stock should not experience blistering at high temperatures.

(e) Flange Design.

A considerable amount of time was wasted in trying to obtain vacuum-tight welds at the points where thermocouple walls, heater casings, etc., entered the heavy top flange, in spite of attempts to reduce the flange metal thickness near these joints. The difficulty is that the heavy cross-section carries away the heat from the weld

too rapidly, requiring excessive local temperatures. To prevent this in the future, all thin-walled tubes entering the casing should first be positioned and welded to a thin plate attached to a pipe section of tapering thickness. The thick part of the pipe could then easily be welded to a thinned section of the flange. Alternatively, a long pipe could be welded to the top flange and the various tubes fastened to a thin plate at the top of the tube above the furnace by silver soldering. By this means, even heaters which might fail could be removed and replaced without disassembling the cell or removing it from the furnace.

(f) Suspension of Emitter.

At present the emitter rests on a bottom Lava support tip and is kept erect by Lava side tips. During assembly of the cell (which must be done with the cell upside down) there is always danger of breaking the bottom tip when the cell is turned erect or is accidentally jarred. There is no way to check whether this has occurred except by making runs and then carefully disassembling to examine the points. Fortunately the bottom points were not found broken when disassembling the cell after each series of runs. However, to eliminate this uncertainty, it would be desirable to hang the emitter-receiver "heart" of the cell from the upper flange by means of thin rods, threaded at both ends for vertical adjustability. The emitter would then hang in the receiver and be supported laterally by the Lava side pieces. There would be no bottom point to break and also heat flow through the bottom support would be eliminated entirely.

V. NOMENCLATURE

a = length of support point (cm or in.)

c_p = specific heat at constant pressure (cal./g. °C)

c_v = specific heat at constant volume (cal./g. °C)

C = cell constant (watt-sec.cm/cal.)

D_{11} = coefficient of self-diffusion

e = eccentricity (cm or in.)

E = e.m.f. (electromotive force)

f = constant in equation (1) (dimensionless)

g = gravitational constant (cm/sec.^{2} or ft./sec.^{2})

k = thermal conductivity (cal./sec. °C cm)

ln = natural logarithm

L = length (cm or in.)

M = molecular weight

P = pressure (atmospheres or dynes/cm^2)

q = heat flow (cal./sec. or watts)

r = radius (cm or in.)

R = gas constant, 1.987 (cal./°C g-mole)

S_1, S_2 = Sutherland constant in equation (10) (°C)

$S_{12} = \sqrt{S_1 S_2}$

t = temperature (°C)

Δt = temperature difference (°C)

T = temperature (°K)

x = clearance at bottom of cell (in.)

α = accommodation coefficient

γ = specific heat ratio, c_p/c_v

δ = annulus width (cm or in.)

η = viscosity, (poise)

ρ = density (g./cm^3)

Subscripts.

1 = inner cylinder (e.g., r_1)

2 = outer cylinder

VI. REFERENCES

1. Andrews, T. Proc. Roy. Irish Acad. 1, 465 (1840).

2. Boltzmann, L. "Vorlesungen uber Gastheorie" Vol. 1, p. 139 (1895).

3. Brewer, L. "The Thermodynamics of High Vacuum - High Temperature Systems Applied to Refractories." Metallurgical Project CC-1802, June 8, 1944 (University of California).

4. Bromley, L. A. "Thermal Conductivity of Gases at Moderate Pressures," University of California Radiation Laboratory Report UCRL-1852, 1952.

5. Bromley, L. A. "Thermal Conductivity of Gases at Moderate Pressures." (Presented at A.I.Ch.E. meeting September 15, 1953, San Francisco.) To be published.

6. Bromley, L. A. and Wilke, C. R. Ind. Eng. Chem. 43, 1641 (1951).

7. Callendar, H. L. Proc. Inst. Civil Engrs. (London) 131 (1897-98).

8. Chapman, S. Phil. Trans. Roy. Soc. (London) A216, 279 (1916).

9. Chapman, S. and Cowling, T. G. "Mathematical Theory of Non-Uniform Gases," University Press, Cambridge (1939).

10. Christiansen, C. Wied. Ann. 14, 23 (1881).

11. Enskog, D. Dissertation, Upsala, 1917.

12. Eucken, A. Physik. Z. 14, 324 (1913).

13. Franck, E. U. Z. Elektrochemie 55, 636 (1951).

14. Gregory, H. S. Phil. Mag. (7) 22, 257 (1936).

15. Gregory, H. S. and Archer, C. T. Phil. Mag. (7) 15, 301 (1933).

16. Gregory, H. S. and Archer, C. T. Proc. Roy. Soc. (London) A110, 91 (1926).

17. Goldschmidt, R. Physik. Z. 12, 418 (1911).

18. Grilly, E. R., Taylor, W. J., and Johnston, H. L. J. Chem. Phys. 14, 435 (1946).

19. Helfgott, A. Physik. Z. 49, 555 (1928).

20. Hercus, E. O. and Laby, T. H. Proc. Roy. Soc. (London) A95, 190 (1918).

21. Hercus, E. O. and Sutherland, D. M. Proc. Roy. Soc. (London) A145, 599 (1934).

22. Hirschfelder, J. O. Bird, R. B. and Spotz, E. L. Chem. Revs. 44, 205 (1949).

REFERENCES

Page 2

23. Hirschfelder, J. O., Bird, R. B. and Spotz, E. L. J. Chem. Phys. 16, 961 (1948).

24. Hirschfelder, J. O., Bird, R. B. and Spotz, E. L. Trans. Am. Soc. Mech. Engrs. 71, 921 (1949).

25. Jakob, Max "Heat Transfer," Vol. I, John Wiley and Sons, New York (1949).

26. Kannuluik, W. G. and Donald, H. B. Australian J. Sci. Research, Ser. A, 3, 417 (1950).

27. Kannuluik, W. G. and Garman, E. H. Proc. Phys. Soc. London 65B, 601, (1952).

28. Kannuluik, W. G. and Martin, L. H. Proc. Roy. Soc. (London) A144, 496 (1934).

29. Kelman, L. R. (Argonne National Laboratory). Communication to A. J. Rothman, Feb. 5, 1952.

30. Kelman, L. R., Wilkinson, W. D. and Yaggee, F. L. "Resistance of Materials to Attack by Liquid Metals." Argonne National Laboratory Report No. ANL-4417, July, 1950.

31. Kennard, E. H. "Kinetic Theory of Gases," New York, McGraw Hill Book Company, 1938.

32. Keyes, F. G. and Sandell, D. J. Trans. Am. Soc. Mech. Engrs. 72, 767 (1950).

33. Keyes, F. G. Trans. Am. Soc. Mech. Engrs. 73, 597 (1951).

34. Keyes, F. G. Tech. Report 37, Project Squid, M. I. T. April 1, 1952. USN and USAF.

35. Kundt, A. and Warburg, E. Pogg. Ann. 156, 177 (1875).

36. Lindsay, A. L. and Bromley, L. A. Ind. Eng. Chem. 42, 1508 (1950).

37. Lyon, R. N. (ed.) "Liquid-Metals Handbook." Atomic Energy Commission and Department of the Navy. Washington, D. C., 1950.

38. McAdams, W. H., "Heat Transmission," 2nd ed., McGraw Hill, New York, 1942.

39. McBain, J. W. "Sorption of Gases by Solids." George Routledge and Sons, London (1932).

40. Maxwell, J. C. Phil. Trans. Roy. Soc. (London) A170, 231 (1879).

41. Michels, A. and Botzen, A., Physica 18, 605 (1952).

REFERENCES

Page 3

42. Northdurft, W. Ann. Physik 28, 137 (1937).

43. Riviere, C. Beibl. Ann. Physik. 6, 867 (1882).

44. Roberts, J. K., Proc. Roy. Soc. (London) 142, 518 (1933).

45. Roeser, W. F. "Temperature, Its Measurement and Control in Science and Industry." (American Institute of Physics), Reinhold, New York, p. 289 (1941).

46. Sandell, D. J. Thesis, Massachusetts Institute of Technology, 1950.

47. Schaefer, K. Z. Physik. Chem. 53, 149 (1943).

48. Sherrat, G. and Griffiths, E. Phil. Mag. 27, 68 (1939).

49. Smithells, C. J. "Metals Reference Book," p. 385. Butterworth Scientific Publications, London (1949).

50. Schleiermacher, A. Wied. Ann. 34, 623 (1888).

51. Stefan, J. Wien. Ber. (IIa) 65, 45 (1872).

52. Stops, D. W. Nature 164, 966 (1949).

53. Stops, D. W. Private communication to L. A. Bromley, Sept. 6, 1950.

54. Stops, D. W. Thesis, London University, 1949 (?)

55. Sutherland, W. Phil. Mag. 40, 421 (1895).

56. Taylor, W. J. and Johnston, H. L. J. Chem. Phys. 14, 219 (1946).

57. Thomas, L. B. and Olmer, F. J. Am. Chem. Soc. 65, 1036 (1943).

58. Trautz, M. and Zink, R. Ann. Physik 7, 427 (1930).

59. Ubbink, J. B. and Haas, W. J. de, Physica 10, 451 (1943).

60. Vargaftig, N. B. Tech. Phys. U.S.S.R. 4, 341 (1937).

61. Vargaftig, N. B. and Oleshchuk, O. M. Izvest. VTI (Vsesoyuz. Teplotekh. Inst.) 15, No. 6, 7 (1946).

62. Vargaftig, N. B. and Parfenov, I. D. Zhur. Eksp. i Teoret. Fiz. (J. Exptl. Theoret. Phys. (U.S.S.R.)) 8, 189 (1938).

63. Wassiljewa, A. Physik. Z. 7, 235 (1938).

REFERENCES

Page 4

64. Archer, C. T. Phil. Mag. 19, 901 (1935)

65. Glassman, I. and Bonilla, C. F. "Thermal Conductivity and Prandtl Number of Air at High Temperatures," p. 458, Preprint, Heat Transfer Symposium, Atlantic City, N. J., Dec. 5, 1951.

VII. APPENDIX

A. Gases Used.

All gases used (except air) were those available commercially in cylinders. No attempt was made to purify the gases, except to pass them through tubes of magnesium perchlorate to dry them. In addition, the liquid carbon dioxide in the cylinder was purified somewhat by opening the valve and blowing off the gas near the top of the cylinder. This procedure lowers the air content of the gas.

Manufacturers' specifications are:

(1) Nitrogen (water-pumped). Linde.
Minimum 99.7% nitrogen
Rare gases (Kr, A, Ne, He) total $<$ 12 p.p.m.

(2) Carbon dioxide. Pure Carbonic.
Minimum 99.5 + % CO_2
Residue chiefly air
Moisture about 40 p.p.m. by volume.

(3) Argon (standard grade). Linde.
Minimum 99.97 + % argon
Residue chiefly nitrogen (about 20-40 p.p.m.)

(4) Helium (grade A). No data available, except "approximately 100% helium, U. S. Navy cylinder."

B. Measurement of Cell Dimensions.

The dimensions necessary for calculation of the cell constant are length, diameters of inner and outer cylinders, and distance of inner cylinder above the bottom of the outer. The inner cylinder diameter was measured by a micrometer at a number of points along its length to ±0.0001". The inside diameter of the outer cylinder was checked using an inside micrometer, but these measurements were considered too crude to use in calculating the annular thickness. Consequently the annulus was determined by the following procedure. The inner cylinder was placed in the outer cylinder with its bottom screwed on. All internal support holes were plugged with paraffin and the annular space was filled to the brim with water measured from a weight buret. The annular thickness was

Table VI

Cell Dimensions

	Cell No. 1 (old)	Cell No. 2 (new)
Emitter length	6.9975"	6.9976"
Emitter diameter:		
average	1.4498"	1.4388"
max. non-uniformity	± 0.00025"	± 0.0005"
Receiver length	7.0273"	7.0422"
Receiver inner diameter	1.5002"*	1.5056"*
Annulus width		
average:	0.0252"	0.03341"**
measurements:	0.0252"	0.03341"
	0.0251	0.03337
	0.0253	0.03345

* Receiver inner diameter obtained from emitter diameter and annulus width.

** After operation at high temperatures the average annulus width was measured and found to be 0.03280 (Cell No. 2B).

calculated from the known length and the diameter of the inner cylinder, and the density of water. The results were reproducible to a few tenths of a percent. In the final measurement of the cell, reproducibility was even better (0.1%) because of improved technique. An innovation was to seal the outer cylinder with stopcock grease to a clear glass plate instead of to the silver bottom. A flashlight was placed at the top and the observer looking up toward the light through the annulus could detect whether air bubbles were present. Only one or two bubbles were found, and their total volume was completely negligible relative to the volume of water in the annulus.

C. Calculation of Cell Constant.

The method of calculating the cell constant is evident from equations 6a, b, c. The only questions arising might be what "average length" is used and how the constant is corrected for temperature.

The average length is determined by (Figure 21):

$$L_{av.} = (1/2)(L_E + L_R) \qquad (13)$$

Note that $L_E + x$ very nearly equals L_R (within ± 0.01").

The temperature variation of the cell constant may be obtained from equations 6a, b, c. The variation with temperature of L is obtained simply by:

$$L_{(\text{at } t°C)} = L_{(\text{at } 22°C)} \left[1 + 20 \times 10^{-6} \ (t-22)\right] \qquad (14)$$

The variation in r is obtained in the same fashion. (20×10^{-6} per °C is the average linear thermal coefficient of expansion of silver and also of stainless steel over the temperature range considered here). The change of x with temperature depends on the difference between the expansion of the silver bottom piece and the Lava spacer. Referring to Figure 21, dimension x is measured at 22°C when the cell is assembled, and a is, of course, known (=0.109"). Since the linear coefficient of

Table VII

Cell Constants

Cell	Temp. °C	x = bottom clearance at 22° C	Cell constant*
1A (old)	50	0.0335"	14,256
1B	50	0.0365"	14,212
	360	"	14,315
	560	"	14,376
1C	370	0.040"	14,266
	470	"	14,298
	570	"	14,329
	680	"	14,365
	770	"	14,391
2 (new)	360	0.041"	10,849
	670	"	10,923
	770	"	10,946

* units: $\left(\frac{\text{watt-sec.-cm.}}{\text{cal.}}\right)$.

expansion of the Lava tip is 3×10^{-6} in./in. per °C,

$$x_t = a \left[1 + 3 \times 10^{-6} (t-22)\right] - (a-x) \left[1 + 20 \times 10^{-6} (t-22)\right], \tag{15}$$

where x_t refers to the space at some temperature t and the unsubscripted x and a refer to values at 22°C.

For convenience in calculating the conductivity in calorie units from heat input measured in watts, the units of the cell constant were made (cm.) (watt-sec./cal.).

D. Sample Run and Calculations.

A typical run, No. 22A, is reproduced in Table VIII. The steady state values are then employed in a sample calculation (Table IX). The method of calculation is evident from sections I-D and VII-C as well as these two tables.

E. Calibration of Thermocouples.

Thermocouples were calibrated by the National Bureau of Standards and by the author. The results are depicted in Figures 22-25, showing the e.m.f. and thermoelectric power (dE/dt) as functions of temperature. Thermoelectric power was obtained by drawing difference plots ($\Delta E/\Delta t$) based on the e.m.f. curves and drawing smooth curves through them.

F. Derivation of Accommodation-Temperature Jump Equation.

1. Derivation Using Gregory's Equation[14] (our Equation (7)).

Consider the concentric cylinder type of apparatus, including the hot wire type of cell. Utilizing equation (7), the correction to be applied to the $\Delta t/q$ measured at one atmosphere to eliminate the effect of accommodation is:

$$\% \text{ correction} = 100 \times \left[\frac{(\Delta t/q)_{1 \text{ atm.}} - \dfrac{\ln (r_2/r_1)}{2\pi kL}}{(\Delta t/q)_{1 \text{ atm.}}} \right] \tag{16}$$

Table VIII

Sample Experimental Run

Run 22A
Nitrogen, 756 mm Hg

Time	Thermocouple Readings, Microvolts			E, millivolts (heater)	Scale Factor	E, millimolts (std. resistor)
	P_{12} (emit.)	Q_{1278} (emit.-rcvr.)	D_{1256} (emit.-guard)			
10:50	Start					
10:58	2994.25	115.8	13.3	71.33	0.6010	47.51
11:05	2993.93	115.8	12.7			
11:15	2993.8	115.75	12.4			
11:25	2993.85	115.8	12.3	71.34	0.6010	47.51
11:30	2993.8	115.8	12.4			
Final Values	2993.8	115.8	12.4	71.335	0.6010	47.51

$$\approx 100 \times \left[\frac{(A/P)(\sqrt{T_1}/r_1 + \sqrt{T_2}/r_2)}{\frac{\ln(r_2/r_1)}{2\pi kL}} \right] \tag{17}$$

This follows from equation (7), if one assumes that the correction to be applied is small, and therefore that the $(\Delta t/q)$, in the denominator of (16) may be replaced by $[\ln(r_2/r_1)/2\pi kL]$. If we restrict our consideration to a single gas, equation (8) becomes:

$$A = \frac{K\ (2-\alpha)}{2\pi L\ \alpha} \tag{18}$$

where $K \equiv \sqrt{\frac{2\pi M}{R}} \cdot \frac{1}{2\ (c_v/R + 1/2)}$ (19)

K thus depends upon gas properties only. Substituting into (17), we get:

$$\%\ \text{correction} \approx 100 \left[\frac{kK(2-\alpha)\ (\sqrt{T_1}/r_1 + \sqrt{T_2}/r_2)}{\alpha \ln (r_2/r_1)} \right] \tag{20}$$

From the form of this equation, it is evident that the correction will be greatest in cases where r_1 (or r_2 or both) are smallest, and where the ratio r_2/r_1 approaches unity. The correction is also highest in cases where the gas has a high molecular weight, high conductivity, and low accommodation coefficient. Also the correction increases with temperature because of the $\sqrt{T}$ term and the fact that α generally decreases with temperature. If we now consider the situation at some fixed temperature, and assume a fixed accommodation coefficient, there are two extreme conditions. The first case is that of the usual hot wire cell in which $r_1 \ll r_2$ and $T_1 \approx T_2$. We find that

$$\%\ \text{correction} \approx \frac{K'}{r_1 \ln (r_2/r_1)} \tag{21}$$

where $K' \equiv \frac{100kK\ (2-\alpha)\sqrt{T_1}}{\alpha}$ (22)

Typical hot wire cell dimensions are those of Gregory and Archer:[15]

Table IX

Sample Calculation (Run 22A)

Heater voltage	= (71.335)(0.6004) = 42.53 volts. (includes corr'n. for voltage drop in std. resistor)
Heater current	= (47.51)(0.01) = 0.4751 amps.
Lead wire correction	= - 0.7%
q (corrected)	= (0.4751)(42.53)(0.993) = 20.21 watts
ΔE (emit.-recvr.)	= 115.8 microvolts
Calibration correction	= 3.0 microvolts
ΔE (corrected)	= 118.8 microvolts
E (average)	= 2937 microvolts
t (average)	= 366° C
dE/dt	= 9.44 microvolts/°C at 366° C
Δt	= 12.58° C
Vacuum correction	= 0.032 watts/°C (from Runs 26 and 27)
$q/\Delta t$	= 1.575 watts/°C (incl. vac. corr'n.)
Pressure correction	= - 0.5% (by extrapolation to 1/P = 0)
Final $q/\Delta t$	= (1.575)(0.995) = 1.567
Cell constant	= 14,315
k	$= \frac{1.567}{14,315} = 10.95 \times 10^{-5}$ cal./(sec.)(°C)(cm.)

$r_1 = 0.0050$ cm, and $r_2 = 0.58$ cm. For this case the calculated percent correction $\approx 42K'$. The second case is that of a cell consisting of concentric cylinders with nearly the same diameters and a relatively small annular width, similar to ours or Keyes and Sandell's.[32,46] Here $r_1 \approx r_2$ and again $T_1 \approx T_2$. Also $r_2/r_1 = 1 + \delta/r_1$, where $\delta = r_2 - r_1$, the width of the annulus. Then $\ln(1 + \delta/r_1) \approx \delta/r_1$, and we get:

$$\% \text{ correction} \approx 2K'/\delta \tag{23}$$

where K' is again defined by (22). The annulus of both our cell and that of Keyes and Sandell is 0.025" or 0.0635 cm, from which it follows that our % correction $\approx 31.5K'$. Thus our corrections are the same order as those for hot wire cells.

2. <u>Derivation from the Temperature Jump Equation</u>.

The basic equation for the temperature jump at the wall of a cell in which the temperature is a function of a linear dimension, r, only (i.e., steady state, one-dimensional heat flow) is:[31]

$$\Delta t_j = g\ (dt/dr) \tag{24}$$

where g = the jump distance, a function of the accommodation coefficient and the mean free path. For radial heat flow in concentric cylinders it is readily shown that:[25]

$$q = -2\pi kLr\ (dt/dr) \tag{25}$$

and

$$q = -2\pi kL\ \frac{\Delta t}{\ln(r_2/r_1)} \tag{26}$$

from which it follows that:

$$dt/dr = \frac{\Delta t}{r\ln\ (r_2/r_1)} \tag{27}$$

The fractional temperature jump effect at each walls is:

$$\frac{\Delta t_j}{\Delta t} = \frac{g}{r_i \ln (r_2/r_1)} \tag{28}$$

where r_i refers to r_1 or r_2 depending upon which wall is bring considered. Again, two cases are recognized. For a hot wire cell, $r_1 \ll r_2$ and so the jump term containing r_1 in the denominator greatly exceeds the one with r_2 in the denominator. Consequently the total jump effect may be considered as equal to that at the wire alone. Thus:

$$\left(\frac{\Delta t_j}{\Delta t}\right)_{total} \approx \frac{g}{r_1 \ln(r_2/r_1)} \tag{29}$$

For the other extreme (e.g., our case), $\ln(r_2/r_1) \approx \delta/r_1$ as before, and for each wall:

$$\frac{\Delta t_j}{\Delta t_o} \approx \frac{g}{\delta} \quad .$$

The form of this equation shows that the jumps at both walls are about the same, so

$$\left(\frac{\Delta t_j}{\Delta t_o}\right)_{total} = \frac{2g}{\delta} \tag{30}$$

These are essentially in the same form as equations (21) and (23) above, except that g replaces K'.

G. Calculation of Conduction Across Supports.

Assume only linear heat flow in the support shown in Figure 26. The cross-sectional area of each cylindrical shell is $dA = 2\pi x dx$. The heat flow through the Lava and air considered as a composite solid is then:[38]

$$dq = \frac{\Delta t \cdot dA}{\frac{y_1}{k_1} + \frac{y_2}{k_2}} = \frac{2\pi x \, \Delta t \, dx}{\frac{y_1}{k_1} + \frac{y_2}{k_2}} \qquad (31)$$

where $\Delta t = t_1 - t_2$. Since $y_2 = R-y$, $y_1 = L - y_2 = L - R + y$, and $y/x = dx/dy$, we get

$$\frac{q}{\Delta t} = 2\pi \int_0^R \frac{y \, dy}{\frac{L - R + y}{k_1} + \frac{R - y}{k_2}} .$$

Rearranging:

$$\frac{q}{\Delta t} = \frac{2\pi k_1 k_2}{k_1 - k_2} \int_0^R \frac{y \, dy}{C' - y} \qquad (32)$$

where

$$C' = R + k_2 L/(k_1 - k_2) \qquad (33)$$

The value of the integral is

$$\int_0^R \frac{y \, dy}{C'-y} = \Big[- y - C'\ln(C'-y) \Big]_0^R = \left[- R - C'\ln \left(\frac{C' - R}{C'} \right) \right]$$

Then

$$\frac{q}{\Delta t} = \frac{2\pi k_1 k_2}{k_1 - k_2} \left[- R - C'\ln \left(\frac{C' - R}{C'} \right) \right] \qquad (34)$$

Substituting the approrpiate quantities:

$k_1 = 0.003$ cal./sec. °C cm

$k_2 = 6.5 \times 10^{-5}$ cal./sec. °C cm

$L = 0.109 \times 2.54 = 0.277$ cm

$R = 0.040 \times 2.54 = 0.1016$ cm

and multiplying by (7)(4.185) to convert to watts and to include the seven supports:

$$q/\Delta t = 0.00254 \text{ (watts/°C)}$$

The net $q/\Delta t$ measured for gas conduction = $(10,200)(6.5 \times 10^{-6}) = 0.924$ (watts/°C), where 10,200 is the cell constant. Then the error in the calculated k due to support conduction = $(0.00254)(100)/(0.924) = +0.28\%$.

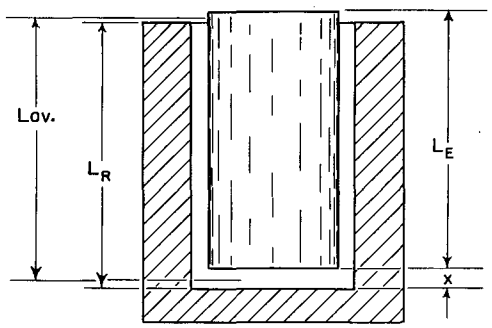

CELL
SCALE HIGHLY EXAGGERATED
$L_{av.} = 1/2\ (L_E + L_R)$

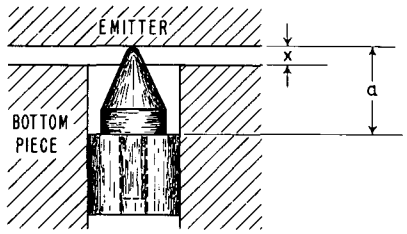

BOTTOM SUPPORT

CELL DIMENSIONS

MU-6204

Figure 21

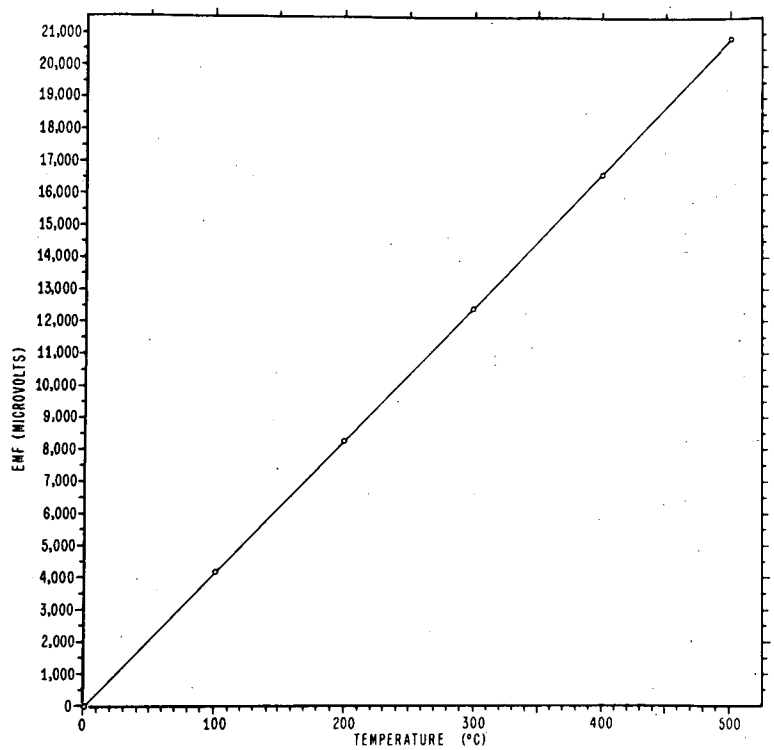

EMF vs. TEMPERATURE CHROMEL-ALUMEL STANDARD THERMOCOUPLE.

MU-6161

Figure 22

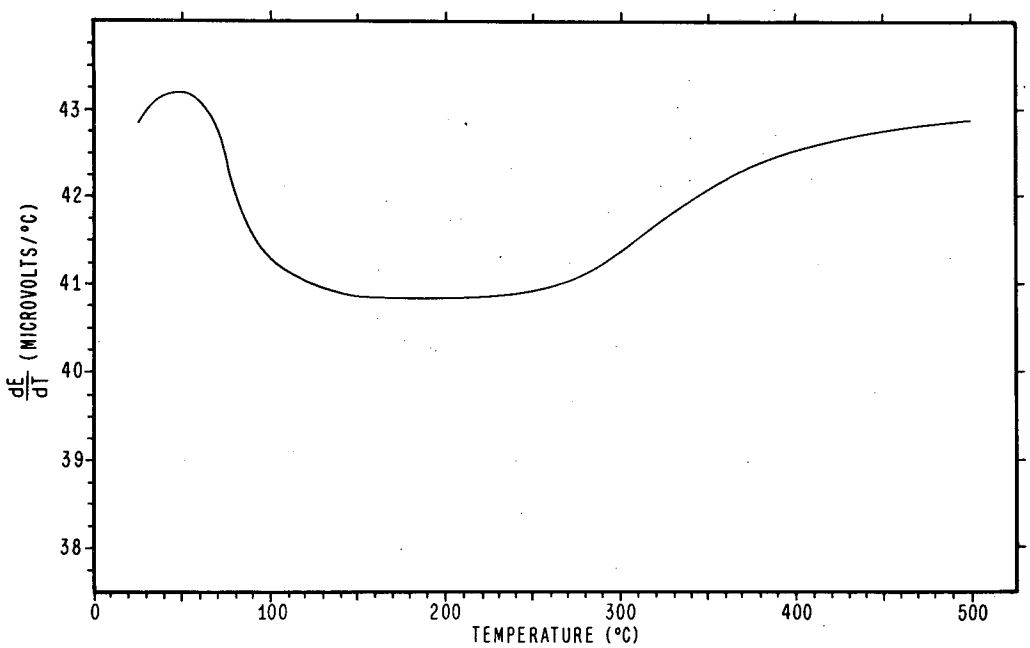

$\frac{dE}{dT}$ vs. TEMPERATURE CHROMEL-ALUMEL STANDARD THERMOCOUPLE.

MU-6159

Figure 23

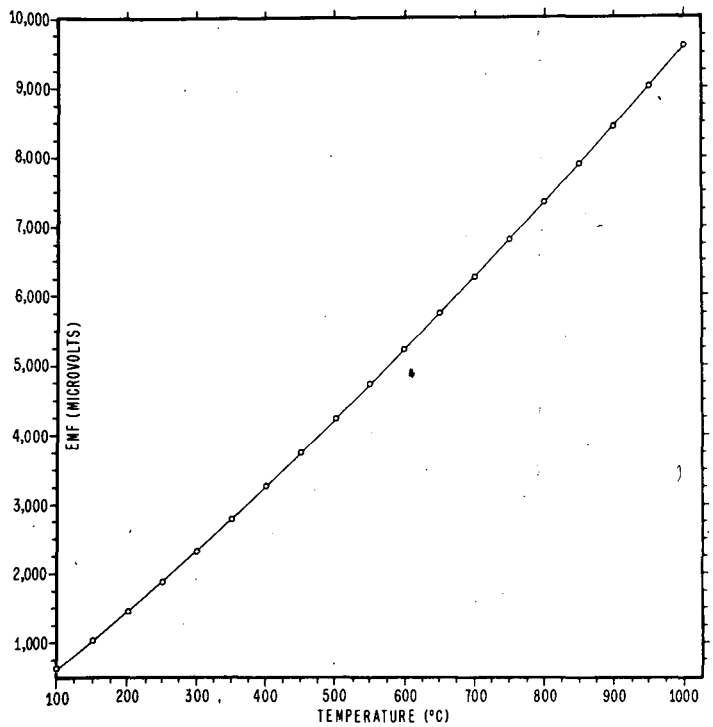

EMF vs. TEMPERATURE PLATINUM – PLATINUM 10% RHODIUM STANDARD THERMOCOUPLE.

MU-6160
21545 1

Figure 24

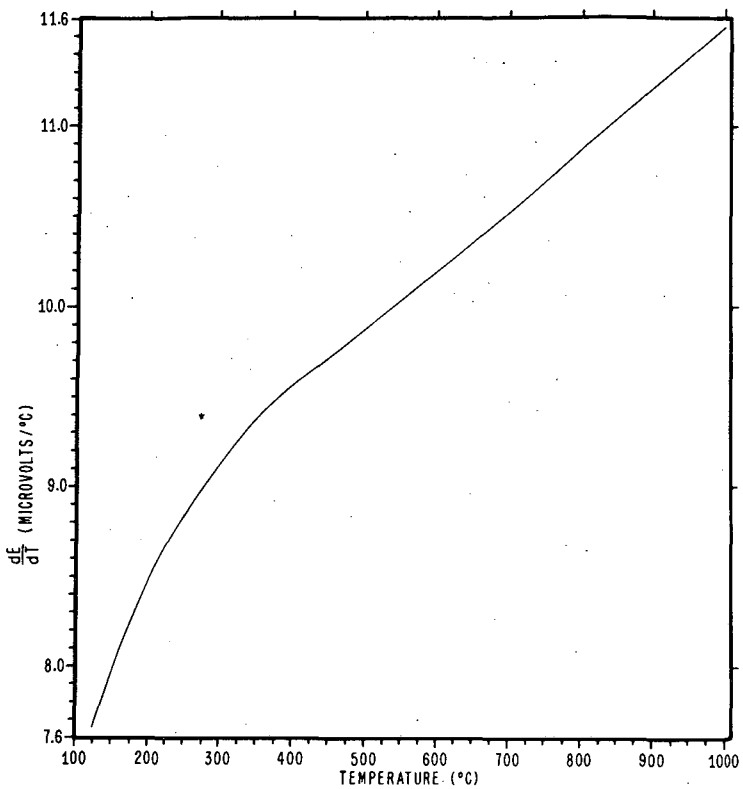

$\frac{dE}{dT}$ vs. TEMPERATURE

PLATINUM-PLATINUM 10% RHODIUM STANDARD THERMOCOUPLE.

MU-6158

21543 1

Figure 25

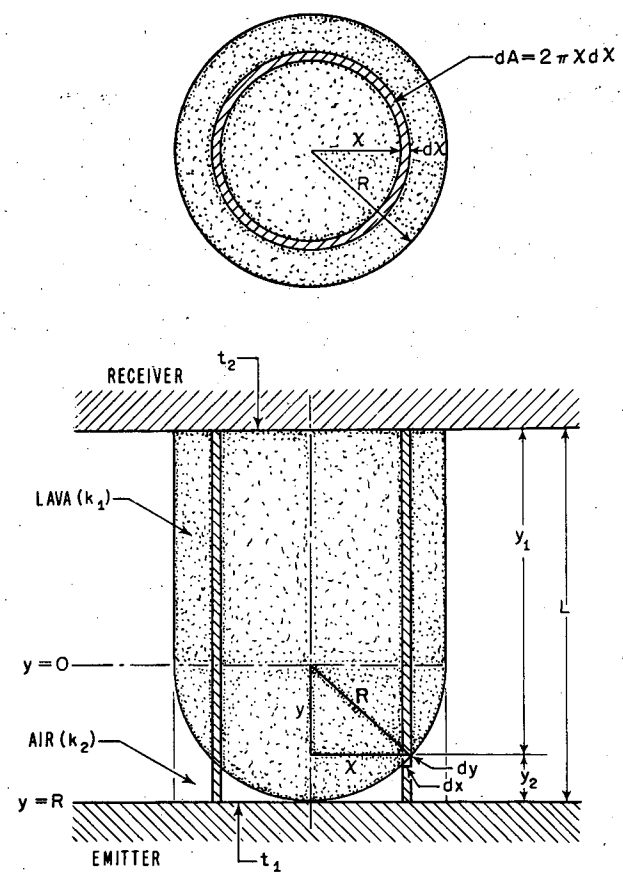

CONDUCTION ACROSS SUPPORT.

MU-6211

Figure 26

ACKNOWLEDGMENT

The author is indebted to Professor LeRoy A. Bromley whose encouragement and advice throughout this investigation was indispensable. Thanks also are offered to the many personnel of the Radiation Laboratory in the shops and clerical offices for their assistance and patience, particularly to Mrs. J. Waite. The aid of Mr. Stephen Whitaker who helped to collect and calculate the data is also appreciated. Finally, thanks are due to the Central Scientific Company who awarded the author a scholarship in 1952-53 during the course of this work.